Turicibacter modifies host bile acids and lipids in a strain-specific manner

Jonathan B. Lynch[1]*, Erika L. Gonzalez[1], Kayli Choy[1], Kym F. Faull[2,3,4,], Talia Jewell[5], Abelardo Arellano[5], Jennifer Liang[5], Kristie B. Yu[1], Jorge Paramo[1], Elaine Y. Hsiao[1]

[1]Department of Integrative Biology & Physiology, University of California Los Angeles, Los Angeles, CA 90095, USA

[2]Department of Psychiatry and Biobehavioral Sciences, University of California, Los Angeles, CA 90095, USA

[3]Jane and Terry Semel Institute for Neuroscience and Human Behavior, University of California, Los Angeles, CA 90095, USA

[4]Pasarow Mass Spectrometry Laboratory, University of California, Los Angeles, CA 90095, USA

[5]Isolation Bio, San Carlos, CA 94070, USA

*Correspondence to: jblynch@g.ucla.edu

ABSTRACT

Bacteria from the *Turicibacter* genus are prominent members of the mammalian gut microbiota and are associated with alterations in dietary fat and body weight, but the specific connections between these symbionts and host physiology are poorly understood. We genomically and phenotypically characterized a diverse set of mouse- and human-derived *Turicibacter* strains, and found they group into three clades that differ in their transformations of bile acids. We identified *Turicibacter* bile salt hydrolases that confer strain-specific differences in bile deconjugation. Colonization with individual *Turicibacter* strains led to changes in host bile acid profiles, generally aligning with those produced *in vitro*. Further, colonizing mice with another bacterium expressing bile-modifying genes from these strains decreased serum cholesterol, triglycerides, and adipose tissue mass. This work identifies genes that enable diverse *Turicibacter* strains to differentially modify host bile acids and lipid metabolism, and positions multiple *Turicibacter* strains as candidates for altering host fat biology.

32 **MAIN TEXT**

33

34 ***Introduction***

35

36 The gut microbiota forms complex relationships with its host organism, modulating broad
37 aspects of host physiology including metabolism[1,2] and neurobiology[3,4]. Often, the connections
38 between the gut microbiota and host physiology are easiest to decipher through presence/absence
39 of large sectors of the microbial community (examples in [5–7]), but in some cases, specific
40 microbial features and/or taxa serve important roles in host physiology[8–10].

41 The bacterium *Turicibacter sanguinis* is the best-studied species of the *Turicibacter*
42 genus, which is prevalent in the gut microbiota of several animals, including humans[11], mice[7],
43 cows[12], pigs[13], and chickens[14]. *Turicibacter* can reach relative abundances of >20% in the rodent
44 small intestine[15] and 0.5% in the human fecal microbiota[16,17]. A study of 1126 sets of twins
45 found *Turicibacter* was a highly heritable taxon in the human fecal microbiota[18], supporting
46 associations between *Turicibacter* abundance and host genetics found in Diversity Outbred
47 mouse collections[19–21]. Long-standing co-evolutionary connections between this taxon and
48 humans are suggested by the high abundance of *Turicibacter* sequences that have been measured
49 in ancient and non-industrial human gut microbiotas[17,22–24].

50 The mammalian gut microbiota has long been associated with obesity[25,26], but studies
51 often provide stronger correlations than mechanistic determinants of these relationships,
52 indicating a further need for fundamental interrogation into connections between the microbiota
53 and host fat[27]. Numerous microbiota community profiling studies reveal correlations between
54 *Turicibacter* and features of host fat metabolism, such as adiposity and dietary lipids[28–33], but the
55 nature of these correlations varies by study[34,35]. We recently observed that the type strain of *T.*
56 *sanguinis,* MOL361[36,37], broadly alters the host serum lipidome while decreasing serum

57 cholesterol and triglycerides in mice[38]. This same strain was also reported to modify certain bile
58 species *in vitro*[21], suggesting at least one potential means by which *Turicibacter* can influence
59 host lipid status. Based on these findings, we hypothesized that there may be variations in the
60 functional activity of *Turicibacter* strains that account for differences in host bile and lipid
61 biology, providing a mechanism to connect this taxon to aspects of host physiology.
62
63 ***Results***
64
65 Turicibacter *isolates separate into genetically distinguishable strains*
66
67 To better understand the diversity within the *Turicibacter* genus, we gathered nine
68 isolates from the fecal microbiotas of mice and humans that had been identified as *T. sanguinis*
69 based on their 16S rRNA gene sequence (97% full length 16S rRNA gene sequence similarity
70 cutoff, **Supplementary Table 1**). Two of these isolates had been previously identified (human-
71 derived type strain MOL361 and H121, which was derived from contaminated germ-free
72 mice[36,39]); five had been isolated but not published (human isolates 18F6, T46, and T129, and
73 mouse isolates 1E2 and TA25); and two were isolated from a human fecal sample specifically
74 for this study (GALT-E2 and GALT-G1) using an array-based isolation and cultivation platform
75 (see Methods). We performed shotgun short read sequencing and created draft assemblies of
76 each isolate genome. Comparisons of the 16S rRNA gene phylogeny (**Fig. 1a**), general genome
77 characteristics (**Fig. 1b**), or specific genome sequence (**Fig. 1c, d**) revealed that even with this
78 fairly small sample of the 16S rRNA gene-based "*T. sanguinis*" species designation, there were
79 at least three distinct subgroups: two from humans (exemplar isolates MOL361 and H121, with
80 99.3% full length 16S rRNA gene similarity), and one from mice (exemplar strain 1E2, 97.5%
81 and 97.8% 16S rRNA gene similarity with MOL361 and H121, respectively). Genomic

82 alignments indicated a substantial amount of shared DNA sequences within members of the
83 same subgroups (within group average nucleotide identity [ANI] all >98.3%) with the remaining
84 amount of genetic variation indicating smaller genetic differences between related isolates. These
85 within-subgroup shared sequences were distinct from members of the other two subgroups
86 (intergroup ANI: MOL361-H121=76.80%, MOL361-1E2=74.95%, H121-1E2=77.43%). It is
87 important to note that the H121-group genomically resembles the newly described species
88 *Turicibacter bilis*[13] (98.8% ANI), currently the only other named species from this genus.
89 Overall, these genomic differences suggest distinct evolutionary histories that correspond at least
90 partially with host origin.
91
92 Turicibacter *isolates differ in their impact on host fat biology and circulating metabolome*
93
94 Previous findings revealed that monocolonizing mice with *T. sanguinis* MOL361 altered
95 host fat tissue and circulating lipids[38]. Due to the large genomic variation between our
96 *Turicibacter* strains, we predicted that they would vary in their effects on host lipid biology. We
97 chose representative isolates from each of the distinct phylogenetic subgroups (MOL361, H121
98 and T129, and 1E2) and measured their effects on circulating metabolites and adipose tissue in
99 monocolonized mice relative to germ-free (GF) and conventionalized controls (*i. e.* gavaged with
100 complete microbiota, CONV). Compared to GF littermates, CONV mice had decreased levels of
101 several dicarboxylate fatty acids, long-chain fatty acids, and long-chain acyl carnitines, with a
102 broad increase in short- and medium-chain acyl carnitines (**Fig. 2a**). Consistent with a previous
103 report[38], colonization with individual *Turicibacter* strains also induced widespread alterations in
104 host serum lipids, with many strain-level differences in host lipid alterations (**Fig. 2a,**
105 **Supplementary Table 2**). Compared to GF controls, MOL361 increased a subset of long-chain
106 acyl carnitines, and decreased many long-chain saturated fatty acids and dicarboxylic acids. In

107 addition, colonization with MOL361 elicited significant decreases in host cholesterol (**Fig. 2b**).
108 Compared to GF, H121 colonization significantly increased serum levels of several medium-
109 chain fatty acids, dicarboxylic acids, and short-, medium- and long-chain acyl carnitines. 1E2
110 colonization had a smaller overall effect on host lipids, but led to a decrease in several
111 dicarboxlyate fatty acids (**Fig. 2a**), At the tissue level, three of the four *Turicibacter* strains
112 stimulated increases in epididymal/gonadal white adipose tissue (e/gWAT) mass in comparison
113 to GF controls, but H121 did not (**Fig. 2c**). Consistent with this, H121 showed the smallest
114 e/gWAT adipocyte size within fat pads (**Supplementary Fig. 1a-f**). This may be due to lower
115 colonization of H121 in both the small intestine and the colon (**Supplementary Fig. 1g, h**)
116 These results indicate that there is not necessarily a connection between changes in specific lipid
117 species and mass of adipose tissue.

118 Bile acids can affect circulating host lipids by altering fat digestion and systemic
119 hormonal signaling[40]. They are produced by the host and released into the small intestine, where
120 they promote digestion of fats by facilitating micelle formation, and can also act through
121 receptors like the farnesoid X receptor (FXR)[40] and GPBAR1/TGR5[41]. Gut bacteria can modify
122 bile acids, primarily through transformations like deconjugation. Previous reports found that
123 MOL361 can broadly modify bile acids *in vitro*[21], so to determine if these abilities allowed
124 MOL361 and other *Turicibacter* strains to modify host bile acids *in vivo*, we profiled serum bile
125 acids in *Turicibacter*-monocolonized mice. Though each strain uniquely impacted host serum
126 metabolites, we noted some patterns in bile acids across monocolonized mice in comparison to
127 either their GF or CONV controls. (Note: bile species with amino acid conjugants are typically
128 referred to as "bile salts," but for simplicity, we will herein refer to both conjugated and
129 unconjugated bile species as "bile acids"). Colonization with MOL361 led to a general decrease
130 in taurine-conjugated primary bile acids (**Fig. 3a**). 1E2 and H121 led to significant increases in
131 glycine-conjugated primary bile acids above normally low levels in GF or CONV mice (**Fig. 3b**).

132 Monocolonization with MOL361, 1E2 and H121 led to increases in the mean levels of
133 unconjugated primary bile acids, with 1E2 and H121 reaching statistical significance (**Fig. 3c**),
134 potentially reflecting bile acid deconjugation by these bacteria. Further, these patterns were
135 largely reflected in levels of individual primary bile acids including conjugated and unconjugated
136 versions of cholate, chenodeoxycholate, and β-muricholate (**Fig. 3d-k**), as well as conjugated
137 and unconjugated secondary bile acid derivatives of ursodeoxycholate, 3-dehydrocholate, and 7-
138 ketodeoxycholate (**Fig. 3l-o**). Importantly, colonization with either MOL361 or, to a less
139 significant extent 1E2, led to decreases in primary and secondary tauro-conjugated bile acids,
140 whereas colonization with H121 or T129 did not (**Fig. 3a, e, h, k, n**). Female mice displayed the
141 most significant *Turicibacter*-associated changes in circulating bile species, lipids, and
142 cholesterol, indicating sex-dependent responses to *Turicibacter* colonization (**Supplementary**
143 **Fig. 2a-c**). This sex difference has also been reported in C57BL/6 mice monocolonized with *T.*
144 *sanguinis* MOL361, albeit with a directionally different change in adipocyte size[38]. Overall,
145 these data demonstrate that colonization with *Turicibacter* differentially alters serum bile acids,
146 lipids, and cholesterol, as well as host fat mass, in a strain-dependent manner.
147
148 Turicibacter *strains differ in their ability to modify host bile acids*
149
150 Based on the large genetic variation between the *Turicibacter* strains (**Fig. 1**) and the
151 differences in serum lipid and bile acid profiles seen in response to colonization with different
152 strains (**Fig. 2**), we posited that these strains differ in their ability to modify bile acids. To test
153 this, we grew each of our nine isolates to stationary phase in rich medium supplemented with a
154 sub-inhibitory concentration of five bile species[21]: cholic acid (CA), chenodeoxycholic acid
155 (CDCA), deoxycholic acid (DCA), taurocholic acid (TCA) and glycochenodeoxycholic acid
156 (GCDCA). We then used liquid chromatography-mass spectrometry (LC-MS) to characterize the

157 resulting bile transformations performed by each isolate (**Fig. 4a**). We discovered that the strains
158 not only differed in their ability to modify this combination of bile species, but also that these
159 capabilities generally mirrored the groupings identified in genomic comparisons (**Fig. 4b**).
160 MOL361, 18F6, and GALT-E2 deconjugated both tauro- and glyco- bile acids, and also
161 dehydrogenated CA and CDCA (**Fig. 4b**). 1E2 and TA25 deconjugated tauro- bile acids, but did
162 not detectably deconjugate glyco- bile acids or perform dehydrogenation (**Fig. 4b**). H121 and
163 T129 deconjugated glyco- bile acids, but did not readily deconjugate tauro- bile acids nor
164 perform detectable dehydrogenation (**Fig. 4b**). T46 and GALT-G1 did not have bile-modifying
165 capacity that mirrored their genetic phylogeny; T46 genomically resembled the MOL361 group
166 but performed modifications similar to the H121 group (*i.e.* glyco- but not tauro- deconjugation,
167 minimal dehydrogenation), whereas GALT-G1, which genomically resembled the H121 group,
168 performed more MOL361-like transformations (*i.e.* glyco- and tauro-deconjugation,
169 dehydrogenation of CDCA) (**Fig. 1, 4b, Supplementary Fig. 3**). Overall, each strain performed
170 at least one of three bile transformations, with some showing capacity for all three (**Fig. 4b,**
171 **Supplementary Fig. 3**).
172 To confirm these intragroup distinctions, we chose one isolate from each of the
173 subgroups (MOL361, H121, 1E2), and grew them in the presence of four primary conjugated
174 bile acids: TCA, taurochenodeoxycholic acid (TCDCA), glycocholic acid (GCA), and GCDCA.
175 This supported the same pattern seen above; MOL361 deconjugated both groups of bile acids,
176 1E2 preferentially deconjugated tauro-conjugates, and H121 preferentially deconjugated glyco-
177 conjugates (**Fig. 4c**). MOL361 and 1E2 displayed broad deconjugation of tauro-conjugates and
178 were able to process at least six taurine-conjugated bile acids (**Fig. 4d**). These data reveal that
179 while all tested strains are efficient modifiers of bile species, their specific transformations differ
180 in a strain-dependent manner, potentially reflecting functions that influence their differential
181 effects on host lipid biology.

182

183 Turicibacter *genomes have different repertoires of bile salt hydrolases*

184

185 The different bile modification abilities across strain subgroups suggested that each
186 contained unique repertoires of bile-modifying genes. We annotated the strain genomes and
187 searched for classes of genes known to perform the deconjugation and dehydrogenation
188 transformations we observed.

189 Certain bacteria from the gut microbiota dehydrogenate hydroxyl groups from the steroid
190 core of bile acids[42], increasing their polarity and modulating their affinity for host bile acid
191 receptors[43]. We searched the *Turicibacter* genomes for homologs of the characterized 7α-
192 hydroxysteroid dehydrogenase (7α-HSDH[21]) from *Clostridium absolum*[44]. This revealed genes
193 with 57% amino acid identity in MOL361, 18F6, T46, and GALT-E2, and homologs with 59%
194 amino acid identity in H121 and T129 (**Supplementary Fig. 4a**). Though the H121-derived
195 putative homolog had higher overall sequence identity than the MOL361-derived homolog, it
196 lacked certain features predicted to be critical for dehydrogenase activity, such as the analogous
197 Asp38 that is catalytically critical for this reaction[44]. Because *in vitro* experiments showed only
198 isolates from the MOL361 group performed bile dehydrogenation, we cloned the putative 7α-
199 HSDH homolog from MOL361 into *E. coli* C41-pLys and then grew these cells in individual
200 unconjugated bile acids that can be dehydrogenated: CA, CDCA, and DCA. Indeed, the protein
201 encoded by the gene removed the mass equivalent of two hydrogens from CA (**Supplementary**
202 **Fig. 4b, c**). Background transformation by *E. coli* prevented clear evidence of CDCA
203 dehydrogenation by this putative 7α-HSDH homolog (**Supplementary Fig. 4d**), but this
204 homolog did not act on DCA (**Supplementary Fig. 4e**), supporting its annotation as a 7α-HSDH.

205 Conjugation increases bile acid solubility and emulsification ability[45], while
206 deconjugation reverses these effects, leading to decreased dietary lipid absorption. To identify

207 *Turicibacter* bile salt hydrolase (*bsh*) genes responsible for the strain-specific differences in bile
208 deconjugation, we first searched our assembled genomes for annotations of "choloylglycine
209 hydrolase," the broad category that includes these genes. Of these annotated genes, we identified
210 eight groups of potentially homologous sequences, and found that each *Turicibacter* strain
211 encodes putative choloylglycine hydrolases from at least two of the eight groups **(Fig. 5a, b**).
212 Isolates within the same phylogenetic and phenotypic subgroups largely shared similar
213 sequences (**Fig. 5a, b**). To assay the function of the strain-specific putative *bsh* genes, we cloned
214 and individually expressed one representative sequence from each of the eight putative
215 choloylglycine hydrolase groups in *E. coli* C41-pLys and measured the ability of these
216 engineered bacteria to perform the deconjugations we observed in our native *Turicibacter*. We
217 cultured the individual *E. coli* strains to stationary phase in the presence of two tauro- (TCA,
218 TCDCA) or glyco- (GCA, GCDCA) bile acids, then measured their ability to deconjugate these
219 bile acid pools. We found that *E. coli* expressing four of the eight putative *bsh* gene groups
220 showed deconjugation activity against at least one of the bile acids (**Fig. 5b-e**). From MOL361,
221 one BSH (group IV) is tauro-specific, and one (group I) deconjugates both glyco- and tauro-
222 conjugates (**Fig. 5c, d**). 1E2 shares a tauro-specific BSH with MOL361 (group IV), and has
223 another BSH (group III) with moderate activity on TCDCA (**Fig. 5c, d**). H121 has a BSH (group
224 II) with activity on TCDCA and GCDCA (**Fig. 5c, d**), although this was blunted when presented
225 with the combined four bile acids (**Fig. 5e**), potentially because of competitive inhibition.
226 Collectively, these findings reveal that *Turicibacter* strains contain a range of bile salt hydrolases
227 with deconjugation preferences for different bile acids.
228
229 *Strain- and substrate-specific bile salt hydrolases from* Turicibacter *differentially alter host lipid*
230 *composition*
231

232 Given that *Turicibacter* colonization broadly modified host lipid and bile pools (**Fig. 2**),
233 and that bile transformations have been previously shown to alter host lipids[46,47], we predicted
234 that expressing *Turicibacter* bile-modifying genes outside the context of *Turicibacter*
235 colonization would be sufficient to impact host lipid biology. To measure the individual effects
236 of these bile acid transformations, we expressed *Turicibacter bsh* genes off of a genomically-
237 integrated high expression vector[48] in the common gut bacterium *Bacteroides thetaiotaomicron*.
238 This bacterium was chosen because it stably colonizes the murine gut, and unlike *E. coli* C41-
239 pLys, contains a homolog of a characterized 7α-HSDH similar to that of *T. sanguinis*
240 MOL361[49,50], allowing the engineered bacteria to more completely mimic *Turicibacter* bile
241 transformations. These strains generally transformed tauro- and glyco- conjugated bile acids as
242 predicted based on the BSH characterization in *E. coli*, including preferential TCDCA
243 transformation, indicating they were capable of performing *Turicibacter*-like bile
244 transformations (**Fig. 6a, Supplementary Fig. 5**). However, the *B. thetaiotaomicron* strain that
245 expressed *bsh* (group III) from strain 1E2 more completely transformed glyco-conjugated bile
246 acids than the strain expressing *bsh* (group II) from H121, counter to the *E. coli* findings. This
247 observation led us to not use the *bsh* (group II)-expressing strain further. Additionally, we
248 noticed *in vitro* growth and bile transformation defects in *B. thetaiotaomicron* expressing *bsh*
249 (group I) from MOL361 (**Supplementary Fig. 6**), that we could compensate for by extending
250 the growth period to better reach cell numbers seen in shorter incubations for the other strains
251 (**Fig. 6b, Supplementary Fig. 5**).
252 We monocolonized mice with the *bsh*-expressing *B. thetaiotaomicron* strains and
253 assessed their circulating lipid profiles and abdominal WAT mass. We found that expressing
254 individual *Turicibacter bsh* genes in the *B. thetaiotaomicron* background was sufficient to
255 significantly alter host colonic bile levels (**Fig. 6c**) and the absolute abundance of 346 circulating
256 lipid species (**Fig. 6d, Supplementary Table 3**). In particular, expression of either the group I or

257 group IV *bsh* led to a decrease in triglycerides (**Fig. 6d, e**). Expressing the tauro-specific *bsh*
258 (group IV) from MOL361 also decreased diacylglycerides (**Fig. 6g**). Expressing the broader
259 specificity *bsh* (group I) from MOL361 also led to a decrease of phosphatidylglycine,
260 phosphatidylserine, and cholesterol (**Fig. 6d-f, h, i**). Despite having broad capacity for
261 transformation, *B. thetaiotaomicron* expressing *bsh* (group III) from 1E2 did not alter host lipid
262 profiles as much as the other strains **(Fig. 6d-i**). On a tissue-level, *bsh*-expression also altered
263 WAT storage in the colonized mice, with the tauro-specific BSH (group IV) significantly
264 reducing WAT mass (**Fig. 6j**). Similar to our findings with *Turicibacter* monocolonization, we
265 also observed a sex difference in BSH responses, with male mice showing more consistent
266 decrease in triglycerides in response to the tauro-specific BSH from MOL361, and females
267 showing more consistent triglyceride responses to the broadly deconjugating BSH
268 (**Supplementary Fig. 7, 8**). In all, these results demonstrated that expressing strain-specific *bsh*
269 genes from *Turicibacter*, especially those able to process the abundant taurine-conjugated bile
270 acids present in the murine intestine, is sufficient to drastically alter host lipid biology.
271
272 ***Discussion***
273
274 Results from this study show that *Turicibacter* bacteria from the mammalian gut
275 microbiota modulate host bile and lipid compositions in a strain-dependent manner. We
276 identified and characterized five novel *Turicibacter* genes capable of performing bile
277 transformations (four *bsh*, one 7α-HSDH), and revealed that expression of individual *bsh* genes
278 is sufficient to broadly and differentially alter host lipid profiles. Further, we found that while
279 bile-transforming genes are present in all our surveyed *Turicibacter* strains, the specific
280 transformation capacity of BSH variants differed by strain in a manner consistent with host
281 environment co-evolution: bile acids in the human gut are a mix of taurine- and glycine-

282 conjugants, whereas murine bile acids are predominantly taurine-conjugants[51,52], providing
283 different bile environments that are preferentially processed by *Turicibacter* strains isolated from
284 their respective gastrointestinal tracts. This close connection between host-specific bile
285 composition and bacterial modifications may be due in part to the bile sensitivity previously
286 exhibited by MOL361 and/or the high abundance of *Turicibacter* in the small intestine, causing
287 these bacteria to more strongly associate with host genes for bile reabsorption and lumenal bile
288 levels than other bile-modifying gut bacteria[21,53–57].

289 This work displays metabolic consequences of colonization by specific gut bacteria and
290 improves the resolution of our understanding connecting specific taxa—in this case, at the strain
291 level—with host physiology. In rodent and human studies, *Turicibacter* relative abundance often
292 negatively correlates with dietary fats[29,31,58–62] and host adiposity[28,33,63], but some studies have
293 shown opposite relationships[30,64,65]. This could be a result of the phenotypic diversity identified
294 here among *Turicibacter* isolates wherein the host may experience different lipid outcomes
295 depending on their own specific *Turicibacter* strains, but could also vary with other features such
296 as host genetics and sex[21,38] (**Supplementary Fig. 2, 7, 8**). Importantly, effects of *Turicibacter*
297 colonization could also be influenced by biogeographic organization of an individual's
298 microbiota; in addition to the specific taxonomic membership, *Turicibacter* positioning in the
299 small and large intestine may affect host consequences from their respective bile modifications
300 by transforming bile pools in either section of the gut tract. Despite genomic and localization
301 differences between them, we found that MOL361 and H121 induced lipid metabolite changes
302 that indicate increases in fatty acid oxidation, suggesting that these strains at least share features
303 that alter host fatty acid metabolism.

304 Further research into *bsh* gene regulation in the *Turicibacter* genus, the relationship
305 between bile and *Turicibacter* colonization and transmission behaviors, as well as the native
306 functionality of the putative BSH and 7α-HSDH homologs we tested, will further explain how

307 these bacteria wields their bile modifications in the intestine. Interestingly, several of the *in vitro*
308 bile transformations, specifically increases in unconjugated bile acids, were generalizable
309 between our *in vitro* characterizations and *Turicibacter* colonization, whereas concurrent *in vivo*
310 increases in certain conjugated bile acids seen during 1E2 and H121 colonization indicate the
311 possibility of more complex interactions between host bile production and *Turicibacter*
312 colonization. The fact that the specificity and activity of the individual BSH homologs differed
313 when expressed in different bacterial backgrounds indicates that other unknown cellular or
314 environmental factors influence the way individual BSH act *in vivo*. This may also include
315 mechanisms that modify the functionality of proteins encoded by the other putative BSH
316 homologs we identified from *Turicibacter* which did not deconjugate the specific tauro- or
317 glyco-conjugated bile acids used in our experiments. These findings may influence the ways that
318 bile-modifying genes can be employed to shape host lipid profiles through microbiota
319 engineering, positioning certain microbial species as more appropriate vectors to impart specific
320 host effects. It will also be informative to determine what other activities performed by
321 *Turicibacter* lead to WAT gain in colonized animals, which contrasted findings from colonizing
322 mice with specific *bsh*-overexpressing strains of *B. thetaiotaomicron*. Given this finding, it is
323 likely that *Turicibacter* also influences host lipids through other mechanisms in addition to the
324 bile transformations we characterized.

325 Our work also connects specific *Turicibacter* members and BSH activity with specific
326 host outcomes. Though some host responses such as broadly decreased triglycerides were
327 consistent across our BSH-recipient mice, the exact lipid and cholesterol responses differed,
328 indicating that the type of deconjugations might have differing connections with host physiology.
329 Further work will continue strengthening the exciting prospect of utilizing *Turicibacter* and/or its
330 bile modifications to intentionally alter host lipid biology to improve host metabolic and lipid-
331 associated health[66,67], as has been proposed with other bacteria[54,68]. Beyond lipid biology,

332 *Turicibacter* abundance has been correlated with diseases such as Parkinson's disease[69] and
333 depression[70], and selective serotonin reuptake inhibitors (SSRIs) have been found to negatively
334 affect *Turicibacter* growth and colonization[71], potentially because they inhibit activity of its
335 unique serotonin transporter[38]. SSRI use is frequently associated with metabolic side effects like
336 weight gain[72,73], and our findings suggests a hypothesis that connects SSRI use and these side
337 effects: SSRI use could diminish gut colonization of bacteria like *Turicibacter*, thus
338 unintentionally altering their impact on host physiology. Future work may develop strategies to
339 reduce interactions between SSRIs and activity of the microbiota, and minimizing the side
340 effects of these drugs and improving host outcomes. In all, these associations further emphasize
341 the importance of understanding mechanisms connecting members of the diverse *Turicibacter*
342 genus to host physiology.
343
344 ***Methods***
345
346 *Mouse husbandry*
347 Adult (6-8 week old) germ-free Swiss Webster mice were used for all animal
348 experiments according to UCLA Institutional Animal Care and Use Committee-approved
349 protocols. Mice were reared in flexible gnotobiotic isolators on a 12h:12h light dark schedule on
350 standard chow (Labdiet 5K52, 22.1%: 16.6%: 61.3% protein: fat: carbohydrate by calories), then
351 were exited to autoclaved filter top cages with autoclaved chow (Labdiet 5010, 28.7%: 13.1%:
352 58.2% protein: fat: carbohydrate by calories) and water. After one day of cage acclimation, the
353 noted *Turicibacter* or *Bacteroides thetaiotaomicron* strain was grown in YCFA medium (see
354 below) overnight, pelleted by centrifugation, and resuspended in 1X PBS. Mice were colonized
355 by a 200μL gavage containing ~10^6 colony-forming units (CFU) of *Turicibacter* or ~10^8 CFU of
356 *B. thetaiotaomicron*. Alternatively, mice were gavaged with the same volume of PBS alone

357 (referred to as germ-free [GF]) or PBS-suspended fecal slurry from a specific pathogen-free
358 adult mouse (referred to as conventionalized [CONV]). Colonization was quantified using strain-
359 specific TuriSERT primers (**Supplementary Table 4)** and quantitative PCR (qPCR) from
360 weight-normalized contents from the distal small intestine and proximal colon after addition of
361 Low Abundance Microbiota Standard (Zymo) and extraction using the Zymo DNA Mini kit
362 (Zymo).
363
364 *Bacterial culturing*
365 *Turicibacter* isolates and *Bacteroides thetaiotaomicron* strains (**Supplementary Table 1**)
366 were cultured in a flexible vinyl chamber (Coy) in an anaerobic 85%/10%/5% nitrogen/carbon
367 dioxide/hydrogen mixture (Airgas). *Turicibacter* was grown on Schaedler's agar (BD
368 Biosciences) or modified YCFA[74] (pH 7.4, per liter: 100mM MOPS, 10g casitone, 2.5g yeast
369 extract, 2g glucose, 2g maltose monohydrate, 2g cellobiose, 44mg $MgSO_4$, 68mg $CaCl_2$, 0.9g
370 NaCl, 10mg hemin, 0.45g K_2HPO_4, 0.45g KH_2PO_4, 4g $NaHCO_3$, 1g cysteine, 1mg resazurin,
371 1.9mL glacial acetic acid, 0.7mL propionic acid, 90μL isobutyric acid, 100uL isovaleric acid,
372 100uL valeric acid, 10mL ATCC vitamin mixture, 0.2% Tween-80) at 37°C. Cells were normally
373 grown without shaking, but when appropriate, *Turicibacter* cultures were anaerobically
374 transferred to sealed Hungate tubes or 1.7mL microcentrifuge tubes and shaken at 225 RPM at
375 37°C.
376 For *B. thetaiotaomicron* growth curves, cultures were grown in YCFA for ~3 days at 37
377 °C to ensure culture saturation, then were diluted 1:100 in 1mL YCFA in plastic culture tubes.
378 Cells were anaerobically cultured without shaking at 37°C until the noted time points, when the
379 cultures were gently shaken and their absorbance was measured with a Ultraspec 10 Cell Density
380 Meter (Biochrom).

381 *Escherichia coli* C41-pLys (Lucigen) was used for characterizing putative bile
382 modification genes, which were expressed off the pET21+ plasmid. *E. coli* was grown
383 aerobically shaking at 37°C C in Luria Broth (LB, 1% NaCl, 1% tryptone, 0.5% yeast extract)
384 supplemented with 100μg mL^{-1} ampicillin. Expression of genes was induced by addition of
385 100μM IPTG.
386
387 *Bacterial isolation and identification*
388 The frozen stool sample was thawed on ice and diluted 1:10 with PRAS anaerobic
389 dilution blank medium (Anaerobe Systems). 100μL of the diluted stool was further diluted to
390 1:1000 with modified YCFA media containing 0.05% bovine bile, 0.2% Tween-80, and 50mM
391 resorufin and loaded on Prospector® system arrays (Isolation Bio, San Carlos, CA, USA)
392 following manufacturer's instructions. The fluorescent green signal of the arrays at time 0 was
393 read on the Prospector® instrument in a Coy anaerobic chamber and the arrays incubated at 37°C
394 in an Anaerobic Systems AS-580 anaerobic chamber (Anaerobe Systems). At 17 and 41 hours of
395 incubation the arrays were scanned again and the decrease in green fluorescence from time 0 was
396 used as an indicator for bacterial growth in the array nanowells. Bacteria from the array were
397 transferred to 96-well transfer plates containing 200μL per well of modified YCFA media,
398 without the addition of 50mM resorufin. The transfer plates were sealed with a gas permeable
399 film and incubated at 37°C in a Mitsubishi AnaeroPack jar with a gas-generating sachet (Remel)
400 for seven days. After incubation, the contents of 538 wells from the transfer plates with visible
401 turbidity were consolidated into secondary 96-well plates, preserved with reduced glycerol, and
402 stored at -80°C until needed. Unless stated otherwise, all stool and isolate manipulations were
403 conducted anaerobically with a 5% CO_2/5% H_2/90% N_2 atmosphere.
404 Genomic DNA was extracted in a 96-well format from the consolidated Prospector®
405 culture plates using the Extract All Kit (Applied Biosystems). 20μL of culture was combined

406 with 20µL of Lysis Solution and incubated for 10 minutes at 95°C, followed by three minutes at
407 room temperature. The DNA was stabilized with the addition of 20µL of DNA Stabilizing
408 Solution and the resulting DNA lysate stored at -20°C until needed.
409
410 *qPCR screening of novel* Turicibacter *isolates*
411 Genomic DNA from 538 isolates was screened for *Turicibacter* 16S and the *Turicibacter*
412 TuriSERT[38] gene using a multiplexed primer set (**Supplementary Table 4**). Each 25µL qPCR
413 reaction mixture had 1µL Extract All lysate, 10µL SYBR Power master mix (Applied
414 Biosystems), 0.5µL of each of the 10µM primers, and 12µL molecular grade water. The reactions
415 were run in a QuantStudio 6 Flex (Thermo Fisher) with a 95°C hold followed by 40 cycles of
416 95°C for 15s, 50°C for 30s, 72°C for 30s. *Turicibacter sanguinis* MOL361 gDNA and water were
417 used as positive and negative controls, respectively.
418
419 *Molecular cloning*
420 *Turicibacter* genes were amplified from template culture lysates with Phusion or Q5
421 DNA polymerase (NEB) and primers designed to amplify denoted *Turicibacter* genes. pET21- or
422 pWW3837[48]-derived expression plasmids were assembled using Gibson assembly (see
423 **Supplementary Table 4** for oligos) for expression in *E. coli* or *Bacteroides thetaiotaomicron*,
424 respectively. Cloned constructs were confirmed through Sanger sequencing prior to functional
425 characterization. pWW3837-derived constructs were cloned into *B. thetaiotaomicron* VPI-5482
426 as previously described[48]. *bsh*-expressing *B. thetaiotaomicron* was compared to *B.*
427 *thetaiotaomicron* containing the original pWW3837 construct (referred to as wild-type *B.*
428 *thetaiotaomicron*).
429
430 *Genome assemblies*

431 Each strain was streaked on Schaedler agar plates and incubated anaerobically, then an
432 individual colony from each isolate was picked into YCFA medium and grown overnight at
433 37°C. DNA was extracted using the Zymo DNA mini kit (Zymo), with bead beating used to lyse
434 cells. Purified genomic DNA was sequenced by MiGS (migscenter.org), and 151bp paired-end
435 sequences were assembled using CLC Genomics Workbench (Qiagen). Genome assemblies have
436 been deposited at NCBI at BioProject PRJNA846348.
437
438 *Whole genome and gene comparisons*
439 anvi'o[75] was used to profile and visualize the different *Turicibacter* strain DNA
440 sequences to locate putative bile salt hydrolase and 7α-HSDH homologs in contig groups,
441 generate variability profiles, and measure gene coverage and detection statistics. Average
442 nucleotide identity (ANI) was calculated using OrthoANIu[76] (available
443 https://www.ezbiocloud.net/tools/ani).
444 Sequences comparisons between 16S rRNA and *bsh* genes/BSH amino acid sequences
445 were performed in CLC Genomics Workbench (Qiagen). 7α-HSDH sequence comparisons were
446 performed using tblastn[77] using the translated amino acid sequence from *Clostridium absonum*[44].
447
448 *Assessment of bile transformations*
449 *In vitro* characterization of bile transformations by engineered *E. coli* or *B.*
450 *thetaiotaomicron* strains were performed by growing cells in respective media conditions
451 described above supplemented with 0.5mM (total combined concentration) of the noted bile
452 species. Cells were grown to stationary phase (shaking at 37°C), then frozen at -80°C until
453 further processing. Cells were then thawed, pelleted (5 minutes at 16,000 x g), and the
454 supernatant was removed to a new microcentrifuge tube. Three volumes of methanol was added,
455 then the mixture was vigorously mixed for 30-60 seconds and incubated (room temperature, 15

456 minutes). Mixtures were centrifuged (5 minutes, 16,000 x g), the supernatant removed to a clean
457 microcentrifuge tube and dried in a vacuum concentrator. The dried residue was treated with
458 methanol/water/formic acid (50/50/0.1, all by volume) then vigorously mixed and centrifuged as
459 described above. Supernatants were transferred to polypropylene HPLC vials, capped, and
460 maintained at 4°C while aliquots (typically 5μL) were injected onto a reversed phase HPLC
461 column (Cadenza CD-C18, 3.0μm, 250 x 2mm, Imtakt) equilibrated in solution A (water/formic
462 acid, 100/0.1, vol./vol.) and eluted (0.2mL minute^{-1}) with an increasing concentration of solution
463 B (acetonitrile/formic acid, 100/0.1, vol./vol.); minute/% B: 0/30, 45/70, 48/100, 50/30, 67/30).
464 The effluent from the column was passed through an electrospray ion source (capillary voltage
465 42V, capillary temperature 275°C, sheath gas flow 15L min^{-1}, spray voltage 5kV, and -15kV
466 conversion dynode with -1.2kV multipliers) connected to a linear ion trap mass spectrometer
467 (Thermo LTQ) scanning from m/z 95-1000 in the positive ion mode. Spectra were recorded and
468 analyzed with instrument-manufacturer supplied software. Confirmation of proposed elemental
469 compositions was achieved using the same chromatography and ion source configuration with
470 the spectra recorded by scanning on an orbitrap mass spectrometer (Thermo LTQ XL).
471 For bile species quantification, an internal spike-in standard of 100mM chenodeoxycholic
472 acid-D4 (CDCA-D4, Sigma) was added to initial culture supernatants as a normalization
473 reference. Area under the curve from reconstructed ion chromatograms was used to quantify the
474 abundances of each species.
475
476 *Serum metabolite analysis*
477 Mice were euthanized with isoflurane and whole blood was collected via cardiac
478 puncture. Blood was allowed to clot in SST Vacutainer tubes (BD) on ice, then centrifuged (4°C,
479 1 minute, 1500 x g). The supernatant was removed and snap frozen in liquid nitrogen. Serum

480 metabolites were analyzed using global metabolomics platform by Metabolon (Morrisville, NC,
481 USA).
482
483 *Circulating lipid analysis*
484 Mice were fasted for 4-6 hours, then euthanized as described above. Blood was collected
485 via cardiac puncture and deposited into anticoagulatory K_2EDTA Vacutainer tubes (BD) on ice.
486 Blood was centrifuged (4^oC, 15 minutes, 2000 x g), then plasma was collected from supernatant
487 and snap frozen in liquid nitrogen. Shotgun lipidomics was performed by the UCLA Lipidomics
488 Core (Los Angeles, CA, USA) with the following protocol. Thawed plasma was pipetted into
489 glass tubes, a mixture of 70 internal standard lipids (Sciex and Avanti) was added, and lipids
490 were extracted using a modified Bligh and Dyer extraction[78]. The pooled organic layers from
491 two extractions were dried in a vacuum concentrator and resuspended in 50/50 (vol./vol.)
492 methanol/dichloromethane plus 10mM ammonium acetate. After transfer to robovials, samples
493 were analyzed with a Sciex 5500 with DMS Device (Lipidyzer Platform) using a targeted
494 acquisition list of 1450 lipid species. The Lipidyzer Differential Mobility device was tuned using
495 the EquiSPLASH LIPIDOMIX standard mixture (Avanti). Data was analyzed using an in-house
496 platform using previously described parameters[79], and quantitative values were normalized to
497 input volume. Statistical significance identification for species to include in heatmap was
498 performed with two-tailed Welch's t-test (p-value cutoff <0.05).
499
500 *Total colonic bile concentration measurement*
501 Mice were colonized and fasted as described above, then upon sacrifice contents from ~1
502 cm of proximal colon were collected into microcentrifuge tubes and snap frozen in liquid
503 nitrogen. Thawed contents were weighed and suspended into water, then total bile levels were
504 measured using the Bile Acid Assay Kit (Sigma). Total bile values were normalized by sample

505 mass, and each sample value was compared to sex-matched littermate controls. Values shown at
506 "0" were below limit of detection.
507
508 *Adipocyte area calculation*
509 After sacrifice, mice epidydimal or gonadal white adipose tissue (e/g WAT) pads were
510 weighed and placed into 4% paraformaldehyde in 1X PBS for 48 hours at 4°C. Fat pads were
511 washed twice in 70% ethanol, then submitted to the UCLA Translational Pathology Core
512 Laboratory (Los Angeles, CA, USA) for paraffin embedding, sectioning, and H&E staining. Ten
513 adipocyte images from each animal (five from each fat pad) were visualized with a 20X
514 objective on an EVOS microscope (Thermo). Adipocyte area for all cells contained entirely
515 within the field of view was automatically measured using the Fiji[80] Adiposoft[81] plug-in (version
516 1.1.16).
517
518 *Statistical analysis*
519 Statistical calculations were performed in in Prism 9.3.1 (Graphpad). Unless otherwise
520 noted, *** = $p<0.0005$, ** = $p<0.005$, * = $p<0.05$, written p-value = $0.05 < 0.2$. Heatmaps were
521 created using the *pheatmap*[82] package in R (version 3.6.3)[83].
522

523 **REFERENCES**

524 1. Schoeler, M. & Caesar, R. Dietary lipids, gut microbiota and lipid metabolism. *Rev.*
525 *Endocr. Metab. Disord.* **20**, 461–472 (2019).

526 2. Wahlström, A., Sayin, S. I., Marschall, H.-U. & Bäckhed, F. Intestinal Crosstalk between
527 Bile Acids and Microbiota and Its Impact on Host Metabolism. *Cell Metab.* **24**, 41–50
528 (2016).

529 3. Sharon, G., Sampson, T. R., Geschwind, D. H. & Mazmanian, S. K. The Central Nervous
530 System and the Gut Microbiome. *Cell* (2016). doi:10.1016/j.cell.2016.10.027

531 4. Fung, T. C., Olson, C. A. & Hsiao, E. Y. Interactions between the microbiota, immune
532 and nervous systems in health and disease. *Nature Neuroscience* (2017).
533 doi:10.1038/nn.4476

534 5. Rabot, S. *et al.* Germ-free C57BL/6J mice are resistant to high-fat-diet-induced insulin
535 resistance and have altered cholesterol metabolism. *FASEB J.* **24**, 4948–4959 (2010).

536 6. Wikoff, W. R. *et al.* Metabolomics analysis reveals large effects of gut microflora on
537 mammalian blood metabolites. *Proc. Natl. Acad. Sci.* **106**, 3698–3703 (2009).

538 7. Yano, J. M. *et al.* Indigenous bacteria from the gut microbiota regulate host serotonin
539 biosynthesis. *Cell* (2015). doi:10.1016/j.cell.2015.02.047

540 8. Ivanov, I. I. *et al.* Induction of Intestinal Th17 Cells by Segmented Filamentous Bacteria.
541 *Cell* **139**, 485–498 (2009).

542 9. Sokol, H. *et al.* Faecalibacterium prausnitzii is an anti-inflammatory commensal
543 bacterium identified by gut microbiota analysis of Crohn disease patients. *Proc. Natl.*
544 *Acad. Sci.* **105**, 16731–16736 (2008).

545 10. Storelli, G. *et al.* Drosophila Perpetuates Nutritional Mutualism by Promoting the Fitness
546 of Its Intestinal Symbiont Lactobacillus plantarum. *Cell Metab.* **27**, 362-377.e8 (2018).

547 11. Kim, C. Y. *et al.* Human reference gut microbiome catalog including newly assembled

548 genomes from under-represented Asian metagenomes. *Genome Med.* **13**, 134 (2021).
549 12. Huang, S. *et al.* The day-to-day stability of the ruminal and fecal microbiota in lactating
550 dairy cows. *Microbiologyopen* **9**, (2020).
551 13. Maki, J. J. & Looft, T. Turicibacter bilis sp. nov., a novel bacterium isolated from the
552 chicken eggshell and swine ileum. *Int. J. Syst. Evol. Microbiol.* **72**, (2022).
553 14. Feng, Y. *et al.* Metagenome-assembled genomes and gene catalog from the chicken gut
554 microbiome aid in deciphering antibiotic resistomes. *Commun. Biol.* **4**, 1305 (2021).
555 15. Mo, J. *et al.* Structural and quantitative alterations of gut microbiota in experimental small
556 bowel obstruction. *PLoS One* **16**, e0255651 (2021).
557 16. Browne, H. P. *et al.* Culturing of 'unculturable' human microbiota reveals novel taxa and
558 extensive sporulation. *Nature* (2016). doi:10.1038/nature17645
559 17. Martínez, I. *et al.* The Gut Microbiota of Rural Papua New Guineans: Composition,
560 Diversity Patterns, and Ecological Processes. *Cell Rep.* **11**, 527–538 (2015).
561 18. Goodrich, J. K. *et al.* Genetic Determinants of the Gut Microbiome in UK Twins. *Cell*
562 *Host Microbe* **19**, 731–743 (2016).
563 19. Benson, A. K. *et al.* Individuality in gut microbiota composition is a complex polygenic
564 trait shaped by multiple environmental and host genetic factors. *Proc. Natl. Acad. Sci.*
565 **107**, 18933–18938 (2010).
566 20. Org, E. *et al.* Genetic and environmental control of host-gut microbiota interactions.
567 *Genome Res.* (2015). doi:10.1101/gr.194118.115
568 21. Kemis, J. H. *et al.* Genetic determinants of gut microbiota composition and bile acid
569 profiles in mice. *PLoS Genet.* (2019). doi:10.1371/journal.pgen.1008073
570 22. Santiago-Rodriguez, T. M. *et al.* Gut Microbiome of an 11th Century A.D. Pre-Columbian
571 Andean Mummy. *PLoS One* **10**, e0138135 (2015).
572 23. Wibowo, M. C. *et al.* Reconstruction of ancient microbial genomes from the human gut.

573 *Nature* **594**, 234–239 (2021).
574 24. Yatsunenko, T. *et al.* Human gut microbiome viewed across age and geography. *Nature*
575 **486**, 222–227 (2012).
576 25. Turnbaugh, P. J. *et al.* An obesity-associated gut microbiome with increased capacity for
577 energy harvest. *Nature* (2006). doi:10.1038/nature05414
578 26. Thaiss, C. A. *et al.* Persistent microbiome alterations modulate the rate of post-dieting
579 weight regain. *Nature* (2016). doi:10.1038/nature20796
580 27. Chadaideh, K. S. & Carmody, R. N. Host-microbial interactions in the metabolism of
581 different dietary fats. *Cell Metab.* **33**, 857–872 (2021).
582 28. Dhakal, S., McCormack, L. & Dey, M. Association of the Gut Microbiota with Weight-
583 Loss Response within a Retail Weight-Management Program. *Microorganisms* **8**, 1246
584 (2020).
585 29. Liu, W. *et al.* Diet- and Genetically-induced Obesity Produces Alterations in the
586 Microbiome, Inflammation and Wnt Pathway in the Intestine of Apc +/1638N Mice:
587 Comparisons and Contrasts. *J. Cancer* **7**, 1780–1790 (2016).
588 30. Li, T.-T. *et al.* Polyunsaturated fatty acids from microalgae Spirulina platensis modulates
589 lipid metabolism disorders and gut microbiota in high-fat diet rats. *Food Chem. Toxicol.*
590 **131**, 110558 (2019).
591 31. Velázquez, K. T. *et al.* Prolonged high-fat-diet feeding promotes non-alcoholic fatty liver
592 disease and alters gut microbiota in mice. *World J. Hepatol.* **11**, 619–637 (2019).
593 32. Jiao, N. *et al.* Gut microbiome may contribute to insulin resistance and systemic
594 inflammation in obese rodents: a meta-analysis. *Physiol. Genomics* **50**, 244–254 (2018).
595 33. Petersen, C. *et al.* T cell–mediated regulation of the microbiota protects against obesity.
596 *Science (80-.).* **365**, (2019).
597 34. Golloso-Gubat, M. J. *et al.* Gut Microbiota and Dietary Intake of Normal-Weight and

598 Overweight Filipino Children. *Microorganisms* **8**, 1015 (2020).
599 35. Chen, X. *et al.* Alteration of the gut microbiota associated with childhood obesity by 16S
600 rRNA gene sequencing. *PeerJ* **8**, e8317 (2020).
601 36. Bosshard, P. P., Zbinden, R. & Altwegg, M. Turicibacter sanguinis gen. nov., sp. nov., a
602 novel anaerobic, Gram-positive bacterium. *Int. J. Syst. Evol. Microbiol.* (2002).
603 doi:10.1099/ijs.0.02056-0
604 37. Maki, J. J., Nielsen, D. W. & Looft, T. Complete Genome Sequence and Annotation for
605 Turicibacter sanguinis MOL361 T (DSM 14220). *Microbiol. Resour. Announc.* **9**, (2020).
606 38. Fung, T. C. *et al.* Intestinal serotonin and fluoxetine exposure modulate bacterial
607 colonization in the gut. *Nature Microbiology* (2019). doi:10.1038/s41564-019-0540-4
608 39. Auchtung, T. A. *et al.* Complete genome sequence of Turicibacter sp. strain H121,
609 isolated from the feces of a contaminated germ-free mouse. *Genome Announc.* (2016).
610 doi:10.1128/genomeA.00114-16
611 40. Russell, D. W. The Enzymes, Regulation, and Genetics of Bile Acid Synthesis. *Annu. Rev.*
612 *Biochem.* **72**, 137–174 (2003).
613 41. Guo, C., Chen, W.-D. & Wang, Y.-D. TGR5, Not Only a Metabolic Regulator. *Front.*
614 *Physiol.* **7**, (2016).
615 42. Ridlon, J. M., Kang, D.-J. & Hylemon, P. B. Bile salt biotransformations by human
616 intestinal bacteria. *J. Lipid Res.* **47**, 241–259 (2006).
617 43. Makishima, M. *et al.* Vitamin D Receptor As an Intestinal Bile Acid Sensor. *Science (80-.*
618 *).* **296**, 1313–1316 (2002).
619 44. Lou, D. *et al.* The three-dimensional structure of Clostridium absonum 7α-hydroxysteroid
620 dehydrogenase: new insights into the conserved arginines for NADP(H) recognition. *Sci.*
621 *Rep.* **6**, 22885 (2016).
622 45. Klaver, F. A. & van der Meer, R. The assumed assimilation of cholesterol by Lactobacilli

623 and Bifidobacterium bifidum is due to their bile salt-deconjugating activity. *Appl.*
624 *Environ. Microbiol.* **59**, 1120–1124 (1993).
625 46. Yao, L. *et al.* A selective gut bacterial bile salt hydrolase alters host metabolism. *Elife*
626 (2018). doi:10.7554/elife.37182
627 47. Joyce, S. A. *et al.* Regulation of host weight gain and lipid metabolism by bacterial bile
628 acid modification in the gut. *Proc. Natl. Acad. Sci.* **111**, 7421–7426 (2014).
629 48. Whitaker, W. R., Shepherd, E. S. & Sonnenburg, J. L. Tunable Expression Tools Enable
630 Single-Cell Strain Distinction in the Gut Microbiome. *Cell* **169**, 538-546.e12 (2017).
631 49. Hylemon, P. B. & Sherrod, J. A. Multiple forms of 7-alpha-hydroxysteroid dehydrogenase
632 in selected strains of Bacteroides fragilis. *J. Bacteriol.* **122**, 418–424 (1975).
633 50. Sherrod, J. A. & Hylemon, P. B. Partial purification and characterization of NAD-
634 dependent 7α-hydroxysteroid dehydrogenase from Bacteroides thetaiotaomicron. *Biochim.*
635 *Biophys. Acta - Lipids Lipid Metab.* **486**, 351–358 (1977).
636 51. Marion, S. *et al.* Biogeography of microbial bile acid transformations along the murine
637 gut. *J. Lipid Res.* **61**, 1450–1463 (2020).
638 52. Hofmann, A. F., Hagey, L. R. & Krasowski, M. D. Bile salts of vertebrates: structural
639 variation and possible evolutionary significance. *J. Lipid Res.* **51**, 226–246 (2010).
640 53. Jones, B. V., Begley, M., Hill, C., Gahan, C. G. M. & Marchesi, J. R. Functional and
641 comparative metagenomic analysis of bile salt hydrolase activity in the human gut
642 microbiome. *Proc. Natl. Acad. Sci.* **105**, 13580–13585 (2008).
643 54. Begley, M., Hill, C. & Gahan, C. G. M. Bile Salt Hydrolase Activity in Probiotics. *Appl.*
644 *Environ. Microbiol.* **72**, 1729–1738 (2006).
645 55. Prete, R. *et al.* Beneficial bile acid metabolism from Lactobacillus plantarum of food
646 origin. *Sci. Rep.* **10**, 1165 (2020).
647 56. Tanaka, H., Hashiba, H., Kok, J. & Mierau, I. Bile Salt Hydrolase of Bifidobacterium

648 longum —Biochemical and Genetic Characterization. *Appl. Environ. Microbiol.* **66**,
649 2502–2512 (2000).
650 57. Kim, G.-B., Miyamoto, C. M., Meighen, E. A. & Lee, B. H. Cloning and Characterization
651 of the Bile Salt Hydrolase Genes (bsh) from Bifidobacterium bifidum Strains. *Appl.*
652 *Environ. Microbiol.* **70**, 5603–5612 (2004).
653 58. Ma, D. *et al.* Ketogenic diet enhances neurovascular function with altered gut microbiome
654 in young healthy mice. *Sci. Rep.* **8**, 6670 (2018).
655 59. Gao, X. *et al.* Correlations between α-Linolenic Acid-Improved Multitissue Homeostasis
656 and Gut Microbiota in Mice Fed a High-Fat Diet. *mSystems* **5**, (2020).
657 60. Everard, A. *et al.* Microbiome of prebiotic-treated mice reveals novel targets involved in
658 host response during obesity. *ISME J.* **8**, 2116–2130 (2014).
659 61. Jung, M.-J. *et al.* Chronic Repression of mTOR Complex 2 Induces Changes in the Gut
660 Microbiota of Diet-induced Obese Mice. *Sci. Rep.* **6**, 30887 (2016).
661 62. Huang, J. *et al.* Supplementation of Bacillus sp. DU-106 reduces hypercholesterolemia
662 and ameliorates gut dysbiosis in high-fat diet rats. *Appl. Microbiol. Biotechnol.* **105**, 287–
663 299 (2021).
664 63. Golloso-Gubat, M. J. *et al.* Gut microbiota and dietary intake of normal-weight and
665 overweight filipino children. *Microorganisms* (2020).
666 doi:10.3390/microorganisms8071015
667 64. Caesar, R., Tremaroli, V., Kovatcheva-Datchary, P., Cani, P. D. & Bäckhed, F. Crosstalk
668 between Gut Microbiota and Dietary Lipids Aggravates WAT Inflammation through TLR
669 Signaling. *Cell Metab.* **22**, 658–668 (2015).
670 65. Martinez-Guryn, K. *et al.* Small Intestine Microbiota Regulate Host Digestive and
671 Absorptive Adaptive Responses to Dietary Lipids. *Cell Host Microbe* **23**, 458-469.e5
672 (2018).

673 66. Jones, M. L., Martoni, C. J. & Prakash, S. Cholesterol lowering and inhibition of sterol
674 absorption by Lactobacillus reuteri NCIMB 30242: a randomized controlled trial. *Eur. J.*
675 *Clin. Nutr.* **66**, 1234–1241 (2012).
676 67. Song, Z. *et al.* Taxonomic profiling and populational patterns of bacterial bile salt
677 hydrolase (BSH) genes based on worldwide human gut microbiome. *Microbiome* **7**, 9
678 (2019).
679 68. Russell, B. J. *et al.* Intestinal Transgene Delivery with Native E.
680 coli Chassis Allows Persistent Physiological Changes. *bioRxiv*
681 2021.11.11.468006 (2021). doi:10.1101/2021.11.11.468006
682 69. Jin, M. *et al.* Analysis of the Gut Microflora in Patients With Parkinson's Disease. *Front.*
683 *Neurosci.* **13**, 1184 (2019).
684 70. Barandouzi, Z. A., Starkweather, A. R., Henderson, W. A., Gyamfi, A. & Cong, X. S.
685 Altered Composition of Gut Microbiota in Depression: A Systematic Review. *Front.*
686 *Psychiatry* **11**, (2020).
687 71. Jackson, M. A. *et al.* Gut microbiota associations with common diseases and prescription
688 medications in a population-based cohort. *Nat. Commun.* (2018). doi:10.1038/s41467-
689 018-05184-7
690 72. Ferguson, J. M. SSRI Antidepressant Medications. *Prim. Care Companion J. Clin.*
691 *Psychiatry* **03**, 22–27 (2001).
692 73. Cascade, E., Kalali, A. H. & Kennedy, S. H. Real-world data on SSRI antidepressant side
693 effects. *Psychiatry* (2009).
694 74. Duncan, S. H. Growth requirements and fermentation products of Fusobacterium
695 prausnitzii, and a proposal to reclassify it as Faecalibacterium prausnitzii gen. nov., comb.
696 nov. *Int. J. Syst. Evol. Microbiol.* **52**, 2141–2146 (2002).
697 75. Eren, A. M. *et al.* Community-led, integrated, reproducible multi-omics with anvi'o. *Nat.*

698 *Microbiol.* **6**, 3–6 (2021).
699 76. Yoon, S.-H., Ha, S., Lim, J., Kwon, S. & Chun, J. A large-scale evaluation of algorithms
700 to calculate average nucleotide identity. *Antonie Van Leeuwenhoek* **110**, 1281–1286
701 (2017).
702 77. Altschul, S. F. *et al.* Gapped BLAST and PSI-BLAST: A new generation of protein
703 database search programs. *Nucleic Acids Research* (1997). doi:10.1093/nar/25.17.3389
704 78. Hsieh, W.-Y., Williams, K. J., Su, B. & Bensinger, S. J. Profiling of mouse macrophage
705 lipidome using direct infusion shotgun mass spectrometry. *STAR Protoc.* **2**, 100235
706 (2021).
707 79. Su, B. *et al.* A DMS Shotgun Lipidomics Workflow Application to Facilitate High-
708 Throughput, Comprehensive Lipidomics. *J. Am. Soc. Mass Spectrom.* **32**, 2655–2663
709 (2021).
710 80. Schindelin, J. *et al.* Fiji: an open-source platform for biological-image analysis. *Nat.*
711 *Methods* **9**, 676–682 (2012).
712 81. Galarraga, M. *et al.* Adiposoft: automated software for the analysis of white adipose tissue
713 cellularity in histological sections. *J. Lipid Res.* **53**, 2791–2796 (2012).
714 82. Kolde, R. pheatmap: Pretty Heatmaps. (2019).
715 83. Team, R. C. R: A language and environment for statistical computing. (2020).
716

717 ***Acknowledgments***

718 *Turicibacter* isolates H121, TA25, T46 and T129 were a gift from Thomas Auchtung. 18F6 and
719 1E2 were a gift from Kenya Honda. pWW3837 and *B. thetaiotaomicron* VPI-5482 was a gift
720 from Fatima Enam and Justin Sonnenburg. We would like to thank Alexander Yoon, Gazmend
721 Elezi, and Lauren Seaman for technical assistance with the LC-MS operation and protocols. This
722 work was supported by funding from the Packard Foundation (E.Y.H.) and Ford Foundation
723 (J.B.L.). E.Y.H. is a New York Stem Cell Foundation – Robertson Investigator. This research
724 was supported in part by The New York Stem Cell Foundation.

725

726 ***Author Contributions***

727 J. B. L., E. L. G, K. C., K. B. Y., J. P. and E. Y. H. conceptualized and planned bacterial and
728 mouse experiments. J. B. L. and K. F. F. designed and performed LC-MS experiments. J. B. L.,
729 T. J., A. A., and J. L. performed isolation and characterization of novel *Turicibacter* isolates. J.
730 B. L. and E. Y. H. wrote manuscript. All authors read and edited final manuscript.

731

732 ***Competing Interests***

733 The authors declare no competing interests. Findings regarding the host effects of *Turicibacter*
734 reported in the manuscript are the subject of provisional patent application 63/288980, owned by
735 UCLA.

736

737 ***Data availability***

738 Metabolomics and lipidomics datasets are attached to this manuscript as supplementary tables.
739 Raw sequencing reads and genome assemblies for *Turicibacter* strains are deposited at NCBI
740 under BioProject ID PRJNA846348.

741

742 ***Availability of materials***

743 Bacterial strains from this work may be obtained through reasonable request to the

744 corresponding author. Certain materials may be restricted by MTA requirements.

745

746 **FIGURES**

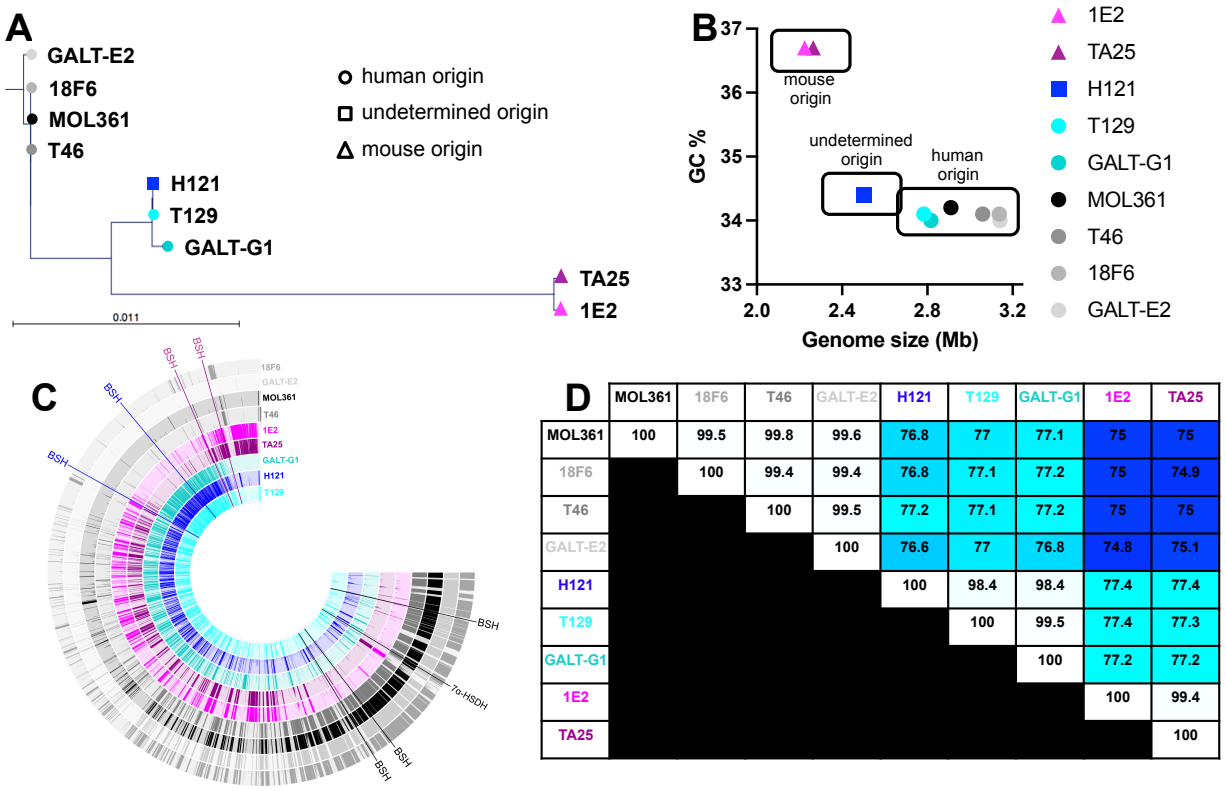

	MOL361	18F6	T46	GALT-E2	H121	T129	GALT-G1	1E2	TA25
MOL361	100	99.5	99.8	99.6	76.8	77	77.1	75	75
18F6		100	99.4	99.4	76.8	77.1	77.2	75	74.9
T46			100	99.5	77.2	77.1	77.2	75	75
GALT-E2				100	76.6	77	76.8	74.8	75.1
H121					100	98.4	98.4	77.4	77.4
T129						100	99.5	77.4	77.3
GALT-G1							100	77.2	77.2
1E2								100	99.4
TA25									100

747

748 **Fig. 1. Genomic comparisons reveal distinct subgroups of *Turicibacter*. a**, Phylogenetic tree
749 comparing full-length 16S rRNA gene sequences from noted *Turicibacter* isolates. Circles
750 indicate human-derived isolates, triangles indicate mouse-derived isolates, and square indicates a
751 mouse-derived contaminating isolate. **b**, Association between guanine-cytosine % (GC%) and
752 calculated genome size in megabases (Mb) for shotgun-assembled genomes of *Turicibacter*
753 isolates from **a**. **c**, Full genome sequence comparisons across *Turicibacter* strains. Position of
754 predicted bile-modification gene homologs are noted outside of rings. Each ring represents
755 sequence blocks in one genome. **d**, Average nucleotide identity (ANI) between noted
756 *Turicibacter* genomes. Number denotes ANI, white to blue scale represents 100%-75% ANI
757 scale.

758

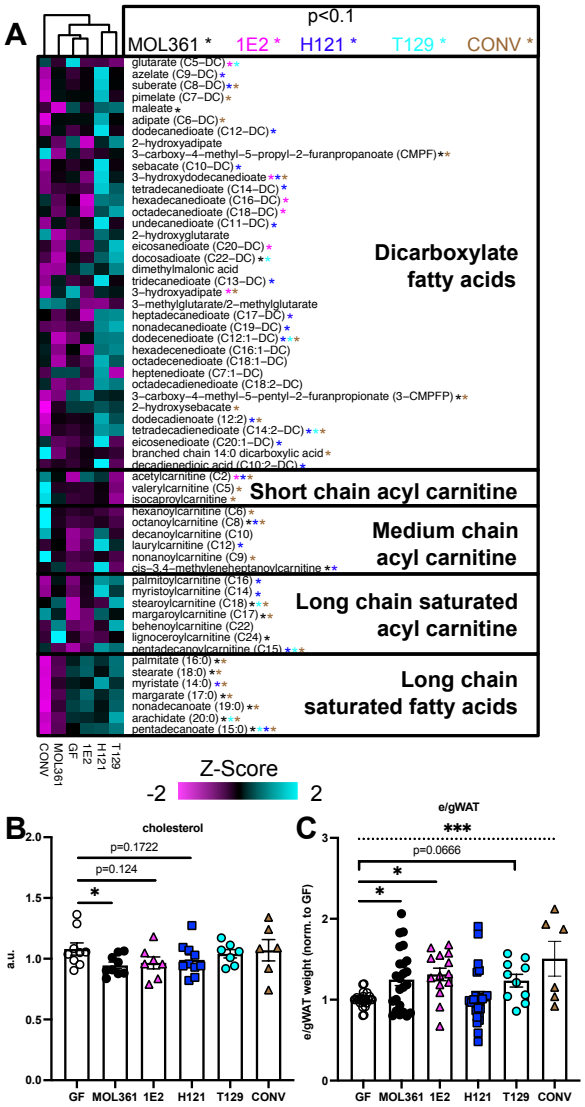

Fig. 2. *Turicibacter* colonization alters host lipids in a strain-dependent manner. a, Heatmap of relative abundance of serum lipids from gnotobiotic mice monocolonized with noted *Turicibacter* strains. Heatmap values represent mean abundance of each detected lipid species from labeled lipid categories scaled across all the means of that individual lipid species. Asterisk (*) colors indicate colonizations with concentrations of that metabolite that are statistically different (p<0.1) from germ-free (GF) animals. **b**, Serum cholesterol concentrations of mice colonized by noted *Turicibacter* strains. **c**, Sex and litter-matched relative epidydimal/gonadal white adipose tissue (e/g WAT) mass of mice monocolonized with noted *Turicibacter* strains. Shapes indicate value for individual mouse, dotted bar represents combined ANOVA statistic for

769 each group versus the experimental mean. Metabolite and cholesterol analysis n=6-10, Welch's

770 two-tailed t-test comparison with GF (false discovery rates compensating for multiple

771 comparisons can be found in **Supplementary Table 2**). WAT analysis n=6-26, Welch's

772 ANOVA test with Dunnet's multiple comparison.*$p<0.05$, ***$p<0.0005$

773

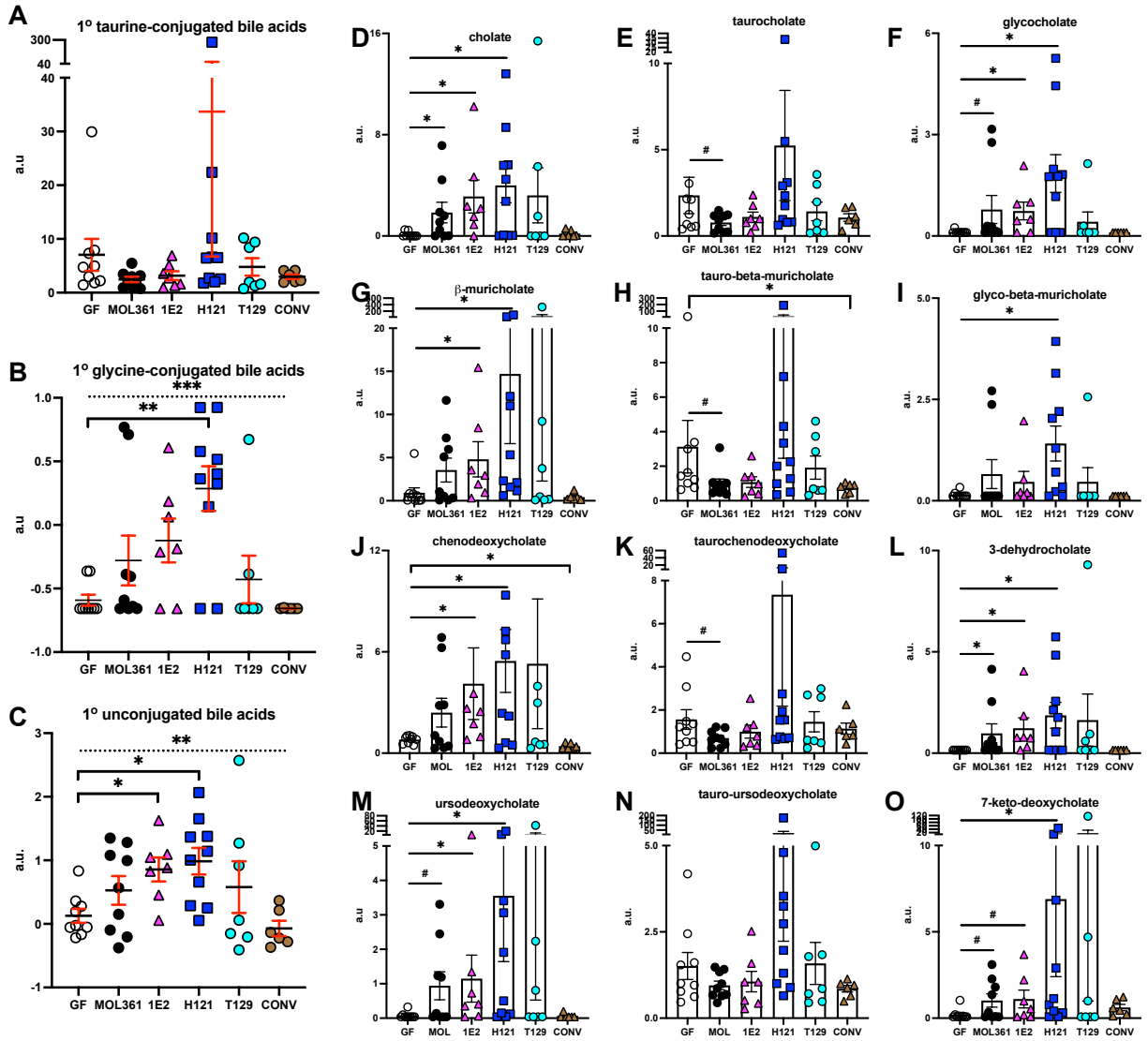

774

775 **Fig. 3. *Turicibacter* colonization alters circulating host bile species. a-c**,: Serum
776 concentrations of pooled primary **a**) taurine-conjugated bile acids, **b**) glycine-conjugated bile
777 acids, or **c**) unconjugated bile acids. **d-o**, Serum levels of individual bile species from mice
778 colonized by noted *Turicibacter* strains. **d, g, j, m** are primary unconjugated bile acids; **e, h, k, m**
779 are primary taurine-conjugated bile acids, **f, i** are primary glycine-conjugated bile acids; **l, o** are
780 secondary unconjugated bile acids. Points indicate value for individual mouse with shapes and
781 colors matching **Fig. 1**, error bars represent mean +/- SEM. Welch's ANOVA with Dunnet's
782 multiple comparison test for combined bile group comparisons, Welch's t-test for individual bile
783 species (multiple comparison false discovery rates presented in **Supplementary Table 2**), n=6-

784 10. Dotted bar represents ANOVA statistic for each group versus the combined experimental

785 mean. #$p<0.1$, *$p<0.05$, **$p<0.005$, ***$p<0.0005$.

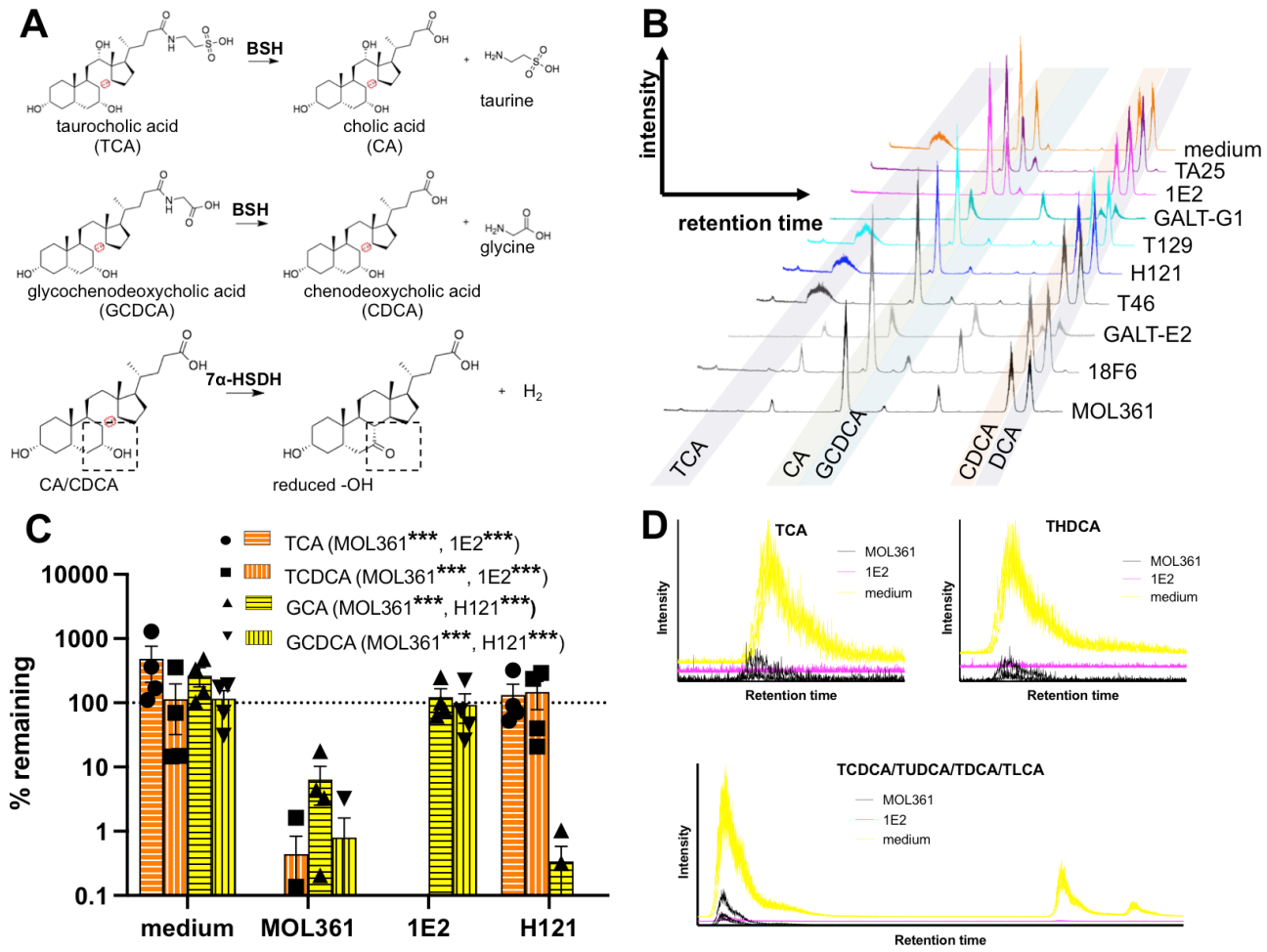

Fig. 4: *Turicibacter* isolates differ in their bile-modifying abilities. a, Schematic for types of bile transformations found to be performed by *Turicibacter* isolates. **b**, Liquid chromatograms of individual *Turicibacter* isolates grown for 24 hours in media with sub-inhibitory concentrations of five bile acids: taurocholic acid (TCA), cholic acid (CA), glycochenodeoxycholic acid (GCDCA), chenodeoxycholic acid (CDCA), and deoxycholic acid (DCA). Shaded regions indicate expected retention time of each bile species. **c**, Percent remaining (compared to cultures at time=0) of conjugated bile acids (TCA, taurochenodeoxycholic acid [TCDCA], glycocholic acid [GCA], GCDCA) after 24 growth with noted *Turicibacter* isolate. Yellow=glycine-conjugated bile acids, orange=taurine-conjugated bile acids. n=4 independent cultures. Values not shown were below 0.1% remaining. Statistical analysis performed by one sample t-test, annotations of legend denotes strains with significant difference from 100% remaining for each

798 bile acid. **d**, Chromatograms of transformation of six taurine-conjugated bile acids (TCA:
799 characteristic m/z range = 461-463; TCDCA, TDCA, TUDCA [tauroursodeoxycholic acid],
800 TLCA [taurolithocholic acid]: characteristic m/z range = 516-518; THDCA
801 [taurohyodeoxycholic acid]: characteristic m/z range = 465-467) after growth with MOL361 or
802 1E2. Each trace represents one biological replicate for that condition, n=3 traces.
803

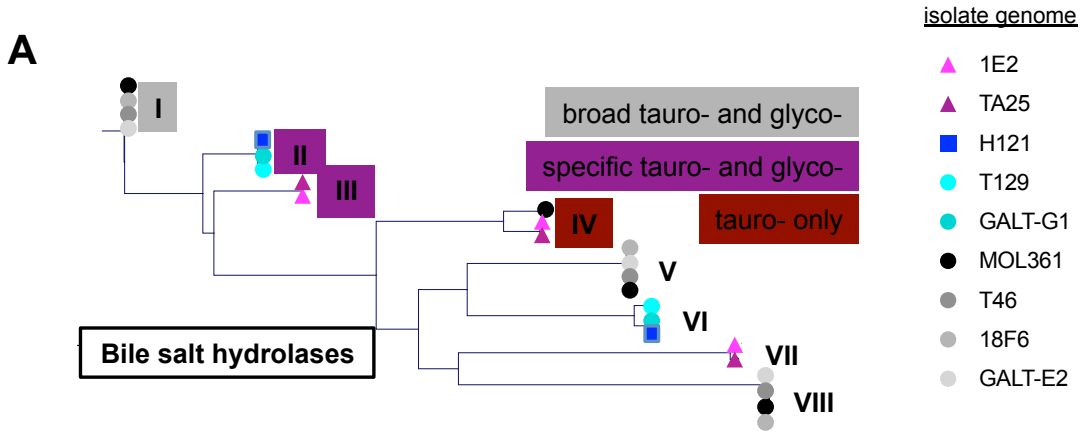

B

Group	I	II	III	IV	V	VI	VII	VIII
MOL361	+			+	+			+
18F6	+				+			+
T46	+				+			+
GALT-E2	+				+			+
H121		+				+		
T129		+				+		
GALT-G1		+				+		
1E2			+	+			+	
TA25			+	+			+	

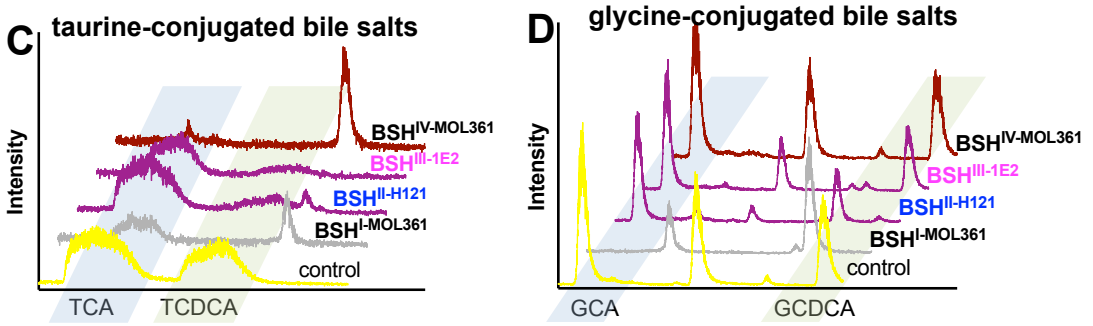

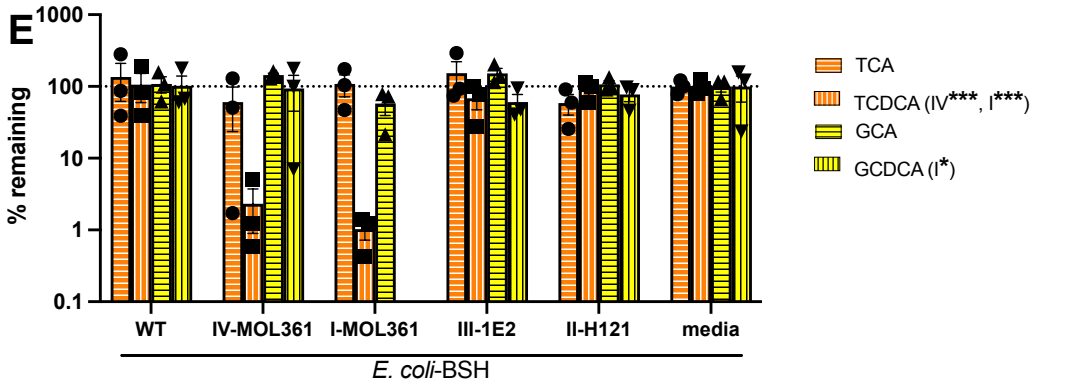

805 **Fig. 5. *Turicibacter* isolates differ in their genetic capacity to modify bile species. a**,
806 Phylogenetic tree of amino acid sequences for each predicted bile salt hydrolase (BSH) sequence
807 from *Turicibacter* strains, with observed bile species specificity noted in boxes. We did not
808 detect bile salt hydrolase activity in sequences without boxes, representing groups V-VIII. **b**,
809 Presence or absence of sequence homologs with potential BSH activity in *Turicibacter* strains. **c**,
810 Liquid chromatograms of media after 24 hour cultures of *E. coli* expressing individual predicted
811 *bsh* genes from each sequence grouping and grown in with TCA and TCDCA. Control is *E. coli*
812 with same expression vector but expressing non-bile-modifying gene. **d**, same as **c**, but with
813 GCA and GCDCA instead of tauro- bile acids. **e**, Quantification of percent remaining (compared
814 to media controls) of conjugated bile acid (TCA, TCDCA, GCA, GCDCA) after 24h growth
815 with *E. coli* expressing the noted *Turicibacter bsh* gene. n=3 independent cultures, *$p<0.05$,
816 **$p<0.005$, ***$p<0.0005$ using one sample t-test comparison with 100% remaining. BSH
817 nomenclature indicates homolog group (*e.g.* III) and isolate of origin (*e.g.* MOL361).
818

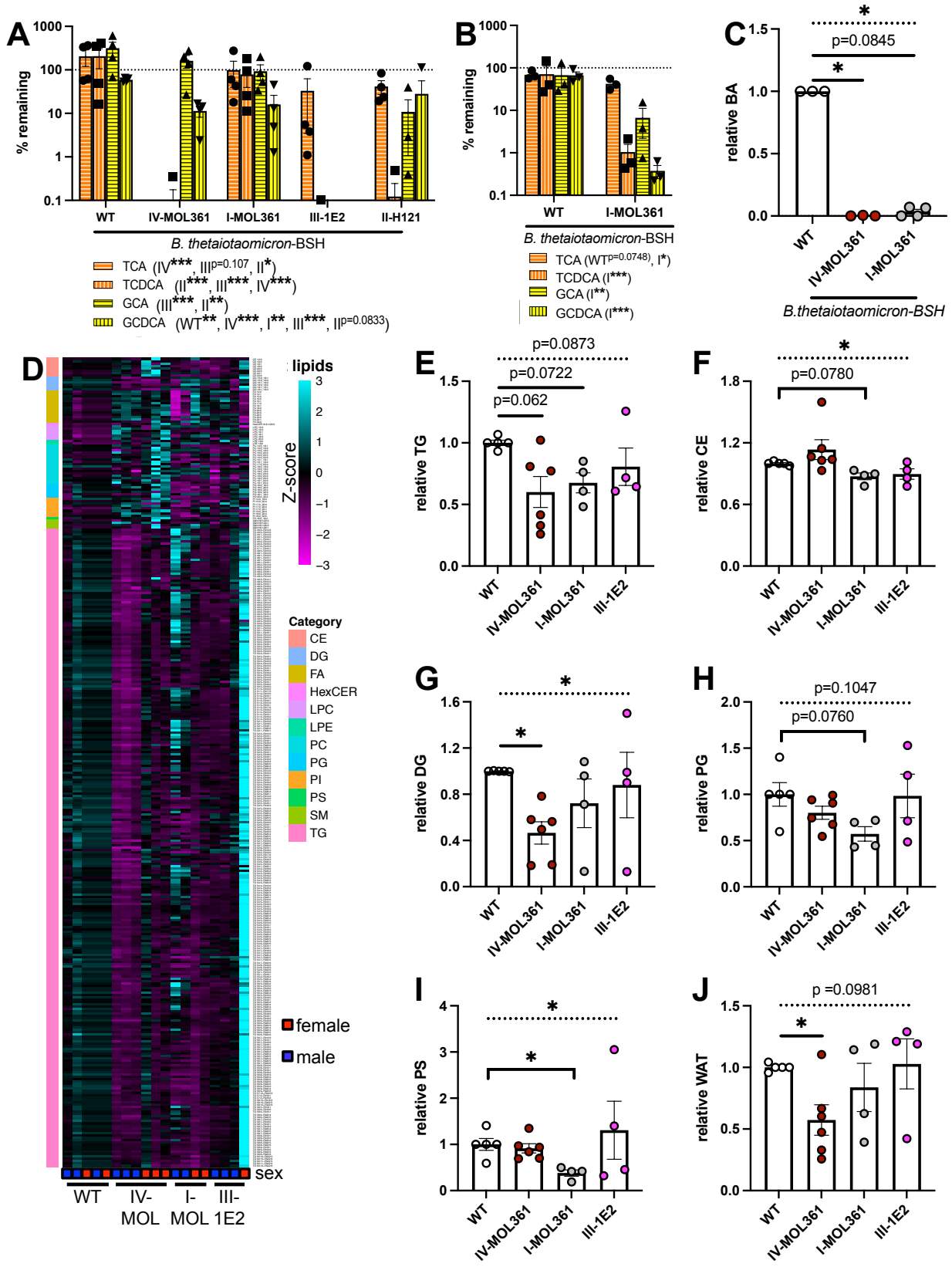
A
% remaining
WT
IV-MOL361
I-MOL361
III-1E2
II-H121
B. thetaiotaomicron-BSH
TCA (IV***, III p=0.107, II*)
TCDCA (II***, III***, IV***)
GCA (III***, II**)
GCDCA (WT**, IV***, I**, III***, II p=0.0833)
B
% remaining
WT
I-MOL361
B. thetaiotaomicron-BSH
TCA (WT p=0.0748, I*)
TCDCA (I***)
GCA (I**)
GCDCA (I***)
C
relative BA
p=0.0845
WT
IV-MOL361
I-MOL361
B.thetaiotaomicron-BSH
D
lipids
Z-score
Category
CE
DG
FA
HexCER
LPC
LPE
PC
PG
PI
PS
SM
TG
female
male
sex
WT
IV-MOL
I-MOL
III-1E2
E
relative TG
p=0.0873
p=0.0722
p=0.062
F
relative CE
p=0.0780
G
relative DG
H
relative PG
p=0.1047
p=0.0760
I
relative PS
J
relative WAT
p =0.0981

819

820 **Fig. 6: *Turicibacter bsh* expression is sufficient to alter host lipidome and health-associated**
821 **lipid markers. a**, Percent remaining of noted bile acids after 24 hour growth with *Bacteroides*
822 *thetaiotaomicron* expressing noted *bsh* genes. n=4 cultures per strain. **b**, Same as **a**, but with 48
823 hour growth with noted *B. thetaiotaomicron* strains. n=3 cultures strain^{-1}. For **a** and **b**, points
824 represent individual comparison with media control, legend annotations denote strains with
825 statistical significance for each bile acid using one sample t-test comparison with 100%
826 remaining. **c**, Quantification of colonic bile acids (BA) from mice colonized with *bsh*-expressing
827 *B. thetaiotaomicron.* Values are normalized to sex-matched littermates colonized with wild-type
828 *B. thetatiotaomicron*. Statistical analysis was performed with Kruskal-Wallis test with Dunn's
829 multiple comparisons test. n=3-4. **d**, Heatmap of circulating lipid species significantly altered by
830 expression of at least one *Turicibacter bsh* in *B. thetaiotaomicron*. Colors on left correspond to
831 lipid class, cyan-magenta color scale represents Z-score, each column represents one animal. **e-i**,
832 Relative combined circulating concentrations of **e**, triglycerides (TG), **f**, cholesterol esters (CE),
833 **g**, diacylglycerides (DC), **h**, phosphotidylglycines (PG), or **i**, phosphotidylserines (PS) of mice
834 monocolonized with *bsh*-expressing *B. thetatiotaomicron.* **j**, Relative white adipose tissue weight
835 of mice monocolonized with *bsh*-expressing *B. thetatiotaomicron*. All values normalized to sex-
836 matched littermates, animal n=4-6 colonization^{-1}, statistical analysis performed by Welch's
837 ANOVA, dotted bar in **c-j** represents ANOVA statistic for each group versus the combined
838 experimental mean. *$p<0.05$, **$p<0.005$, ***$p<0.0005$
839

840 **SUPPLEMENTARY FIGURES**

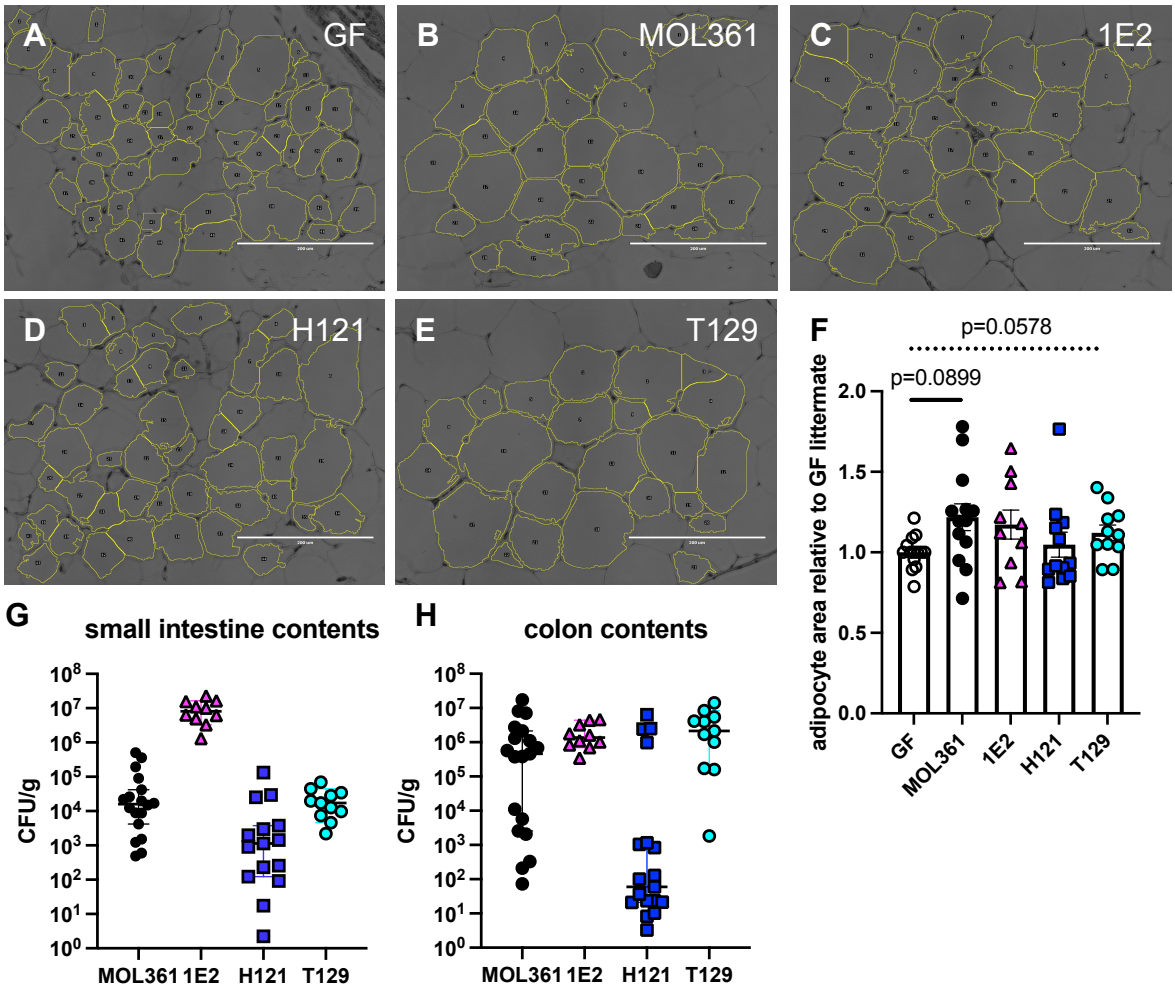

841

842 **Supplementary Fig. 1. Strain-dependent variation in colonization and adipocyte size. a-e**,
843 Representative images of adipose tissue from *Turicibacter* monocolonized mice. **f**, Sex- and
844 litter- matched relative adipocyte area of mice monocolonized with individual *Turicibacter*
845 strains. Each point represents mean of 10 images of adipocyte area per animal. **g, h**, Colony-
846 forming units (CFU) per gram of contents for distal small intestine (**g**) or proximal colon **(h).**
847 Each dot represents sample from one animal, per colonization n=10-15 for qPCR, n=10-14 for
848 adipocyte area calculation. Statistics for adipocyte area performed by Welch's ANOVA with
849 Dunnet's multiple comparisons, dotted bar represents ANOVA statistic for each group versus the
850 combined experimental mean.

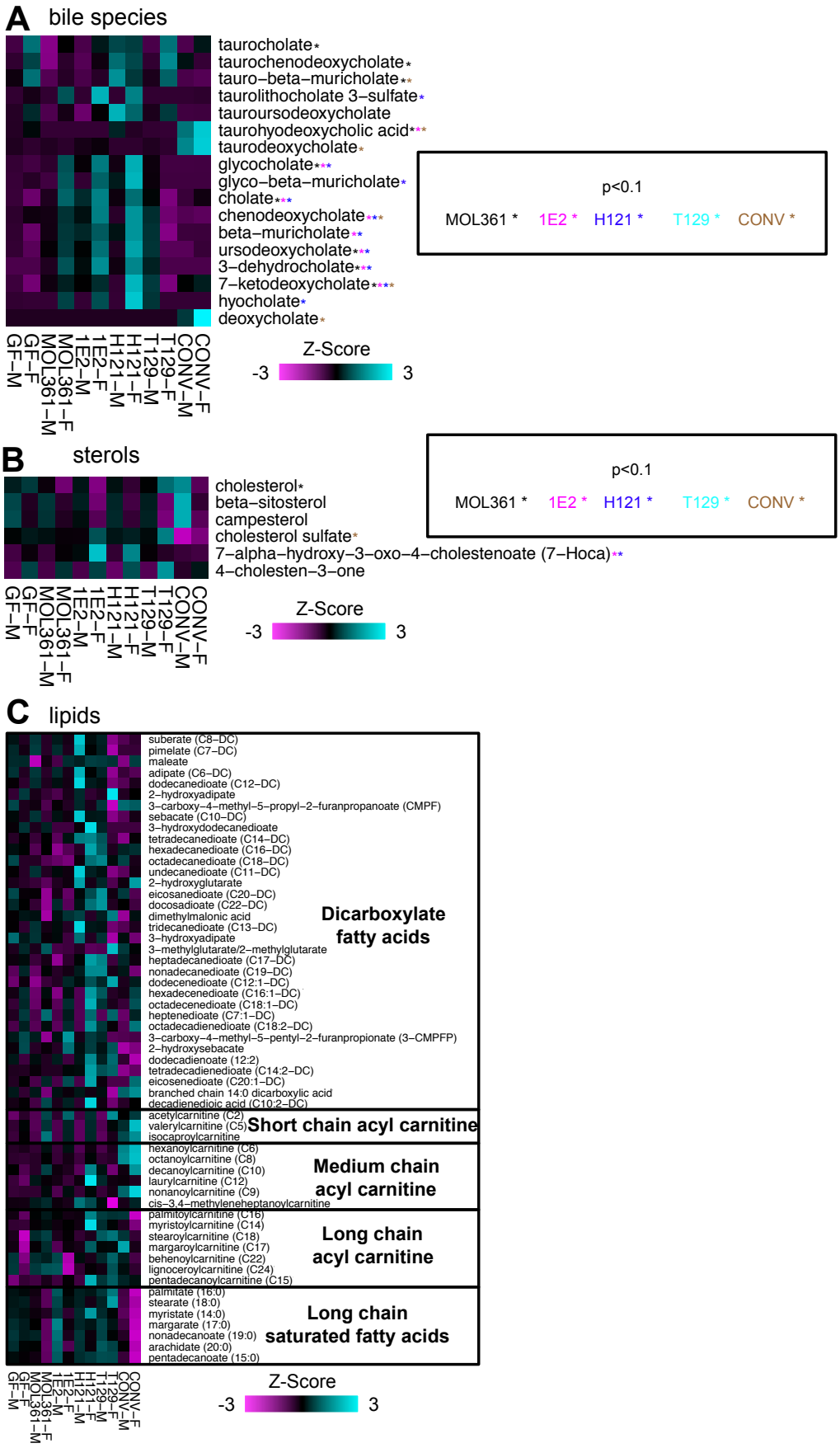
A bile species
taurocholate*
taurochenodeoxycholate*
tauro−beta−muricholate**
taurolithocholate 3−sulfate*
tauroursodeoxycholate
taurohyodeoxycholic acid***
taurodeoxycholate*
glycocholate***
glyco−beta−muricholate*
cholate***
chenodeoxycholate***
beta−muricholate**
ursodeoxycholate***
3−dehydrocholate***
7−ketodeoxycholate****
hyocholate*
deoxycholate*
GF−M
GF−F
MOL361−M
MOL361−F
1E2−M
1E2−F
H121−M
H121−F
T129−M
T129−F
CONV−M
CONV−F
Z-Score
-3
3
p<0.1
MOL361 *
1E2 *
H121 *
T129 *
CONV *
B sterols
cholesterol*
beta−sitosterol
campesterol
cholesterol sulfate*
7−alpha−hydroxy−3−oxo−4−cholestenoate (7−Hoca)**
4−cholesten−3−one
GF−M
GF−F
MOL361−M
MOL361−F
1E2−M
1E2−F
H121−M
H121−F
T129−M
T129−F
CONV−M
CONV−F
Z-Score
-3
3
p<0.1
MOL361 *
1E2 *
H121 *
T129 *
CONV *
C lipids
suberate (C8−DC)
pimelate (C7−DC)
maleate
adipate (C6−DC)
dodecanedioate (C12−DC)
2−hydroxyadipate
3−carboxy−4−methyl−5−propyl−2−furanpropanoate (CMPF)
sebacate (C10−DC)
3−hydroxydodecanedioate
tetradecanedioate (C14−DC)
hexadecanedioate (C16−DC)
octadecanedioate (C18−DC)
undecanedioate (C11−DC)
2−hydroxyglutarate
eicosanedioate (C20−DC)
docosadioate (C22−DC)
dimethylmalonic acid
tridecanedioate (C13−DC)
3−hydroxyadipate
3−methylglutarate/2−methylglutarate
heptadecanedioate (C17−DC)
nonadecanedioate (C19−DC)
dodecenedioate (C12:1−DC)
hexadecenedioate (C16:1−DC)
octadecenedioate (C18:1−DC)
heptenedioate (C7:1−DC)
octadecadienedioate (C18:2−DC)
3−carboxy−4−methyl−5−pentyl−2−furanpropionate (3−CMPFP)
2−hydroxysebacate
dodecadienoate (12:2)
tetradecadienedioate (C14:2−DC)
eicosenedioate (C20:1−DC)
branched chain 14:0 dicarboxylic acid
decadienedioic acid (C10:2−DC)
Dicarboxylate fatty acids
acetylcarnitine (C2)
valerylcarnitine (C5)
isocaproylcarnitine
Short chain acyl carnitine
hexanoylcarnitine (C6)
octanoylcarnitine (C8)
decanoylcarnitine (C10)
laurylcarnitine (C12)
nonanoylcarnitine (C9)
cis−3,4−methyleneheptanoylcarnitine
Medium chain acyl carnitine
palmitoylcarnitine (C16)
myristoylcarnitine (C14)
stearoylcarnitine (C18)
margaroylcarnitine (C17)
behenoylcarnitine (C22)
lignoceroylcarnitine (C24)
pentadecanoylcarnitine (C15)
Long chain acyl carnitine
palmitate (16:0)
stearate (18:0)
myristate (14:0)
margarate (17:0)
nonadecanoate (19:0)
arachidate (20:0)
pentadecanoate (15:0)
Long chain saturated fatty acids
GF−M
GF−F
MOL361−M
MOL361−F
1E2−M
1E2−F
H121−M
H121−F
T129−M
T129−F
CONV−M
CONV−F
Z-Score
-3
3

853 **Supplementary Fig. 2. Host effects of *Turicibacter* colonization varies with sex. a-c**, Heatmap
854 of mean relative **a**) bile species, **b**) sterols, or **c**) lipids. Column labels represent colonization
855 state and sex, M=male, F=female. n=3-6 group^{-1}, except female T129 (n=1). * represents
856 statistical difference of $p<0.1$ between that colonization state (both males and females) compared
857 to GF using Welch's two-sample t-test.
858

	Presence (+) or absence (-) of peak							Deconjugation ability
Turicibacter strain	TCA	Dehydrogenated CA	CA	GCDCA	Dehydrogenated CDCA	CDCA	DCA	
MOL361	-	+	+	-	+	+	+	Tauro- and glyco-deconjugation; dehydrogenation
18F6	-	+	+	-	+	+	+	
GALT-E2	-	+	+	-	+	+	+	
T46	+	-	+	-	-	+	+	Glyco-deconjugation
H121	+	-	+	-	-	+	+	
T129	+	-	+	-	-	+	+	
GALT-G1	-	-	+	-	+	+	+	Tauro- and glyco-deconjugation; some dehydrogenation
1E2	-	-	+	+	-	+	+	Tauro- deconjugation
TA25	-	-	+	+	-	+	+	

Red = outliers from genomic group

Supplementary Fig. 3. Summary table of bile transformations performed by *Turicibacter* isolates. Table indicating presence/absence of noted bile species after growth in mixture of bile acids described in **Fig. 4b**.

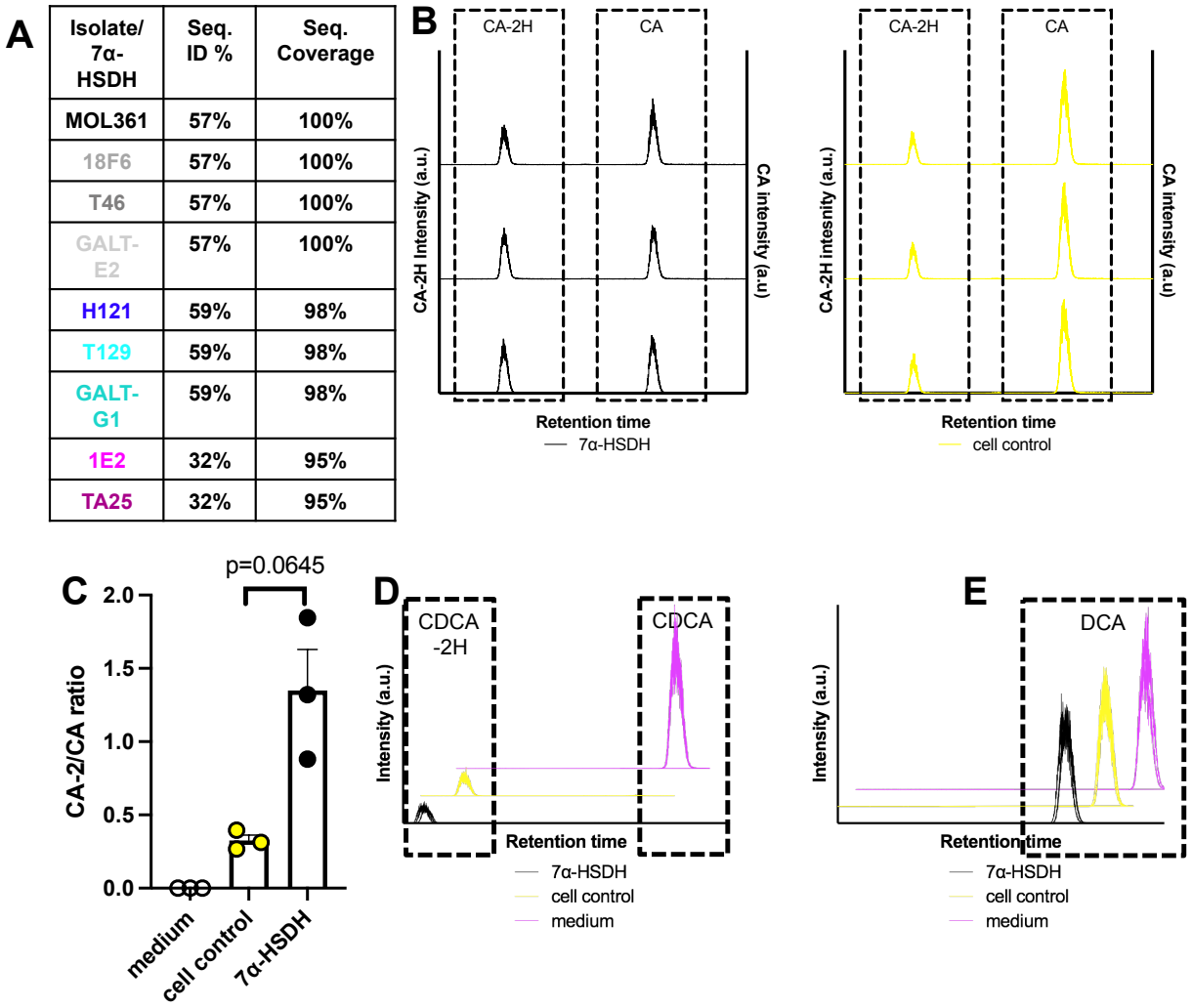

Supplementary Fig. 4. Some strains of *Turicibacter* encode a functional 7alpha-HSDH gene. **a**, Table depicting amino acid similarity and sequence coverage between closest predicted 7alpha-HSDH homolog in noted isolate genome and 7alpha-HSDH gene from *Clostridium absonum*. **b**, Chromatograms of cholic acid (CA) or cholic acid with 2 hydrogens removed (CA-2H) from *E. coli* cultures expressing the MOL361 HSDH homolog (7alpha-HSDH) or non-bile modifying gene sequence in the same plasmid (cell control). Chromatograms from independent triplicate cultures are shown, dotted boxes indicate each bile species. **c**, Quantification of CA/CA-2H ratios determined from reconstructed areas under the curve in **b**. Statistical comparison performed with Welch's t-test, n=3 cultures, bars indicate mean +/- SEM. **d**, Same as **b**, but with CDCA instead of CA. **e**, same as **b**, but with DCA instead of CA. **d** and **e** triplicate

875 chromatograms are stacked on the same axis.

876

Bile salt hydrolase (*bsh*) gene	Presence (+) or absence (-) of peak				Deconjugation ability
	TCA	TCDCA	GCA	GCDCA	
I-MOL361	-	-	-	-	Tauro- and glyco-deconjugation
II-H121	+	-	+	-	-CDCA deconjugation
III-1E2	+	-	+	+	TCDCA deconjugation
IV-MOL361	-	-	+	+	Tauro- deconjugation

877

878 **Supplementary Fig. 5. Bile transformations performed by *B. thetaiotaomicron* expressing**
879 ***Turicibacter bsh* genes.** Table indicating presence/absence of noted bile species after growth in
880 mixture of bile acids described in **Fig. 6a, b**.

881

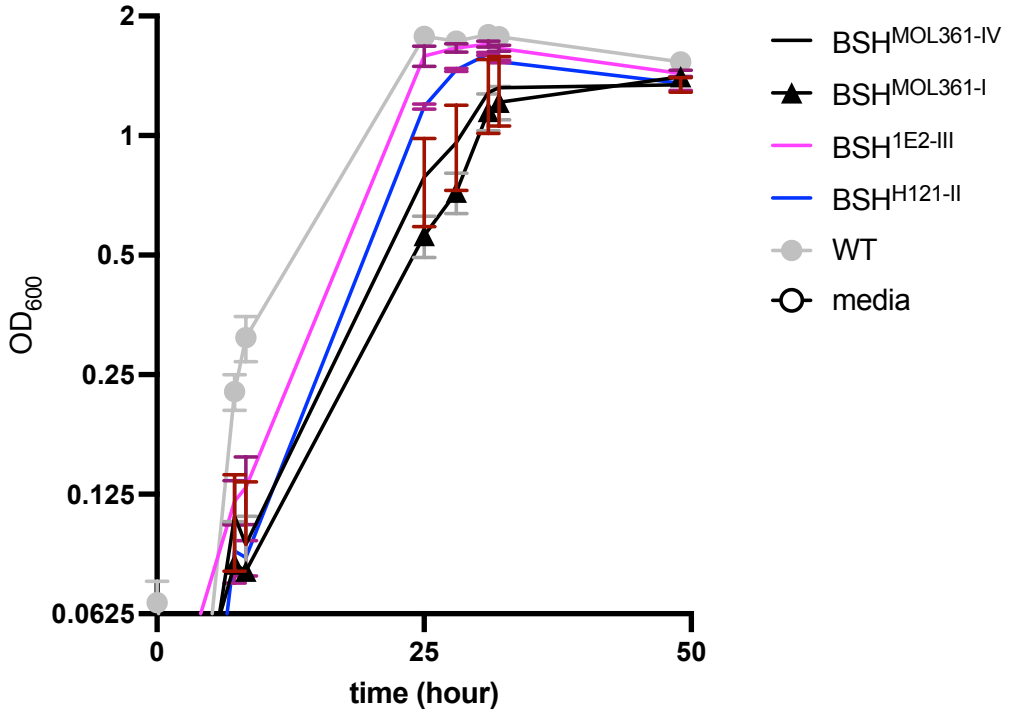

882

883 **Supplementary Fig. 6. Expressing *bsh* genes from *Turicibacter* leads to slight growth defect**

884 **of *B. thetaiotaomicron*.** OD_{600} readings of noted *B. thetaiotaomicron* strains in YCFA medium.

885 Each point represents mean +/- SEM for 3 independent cultures.

886

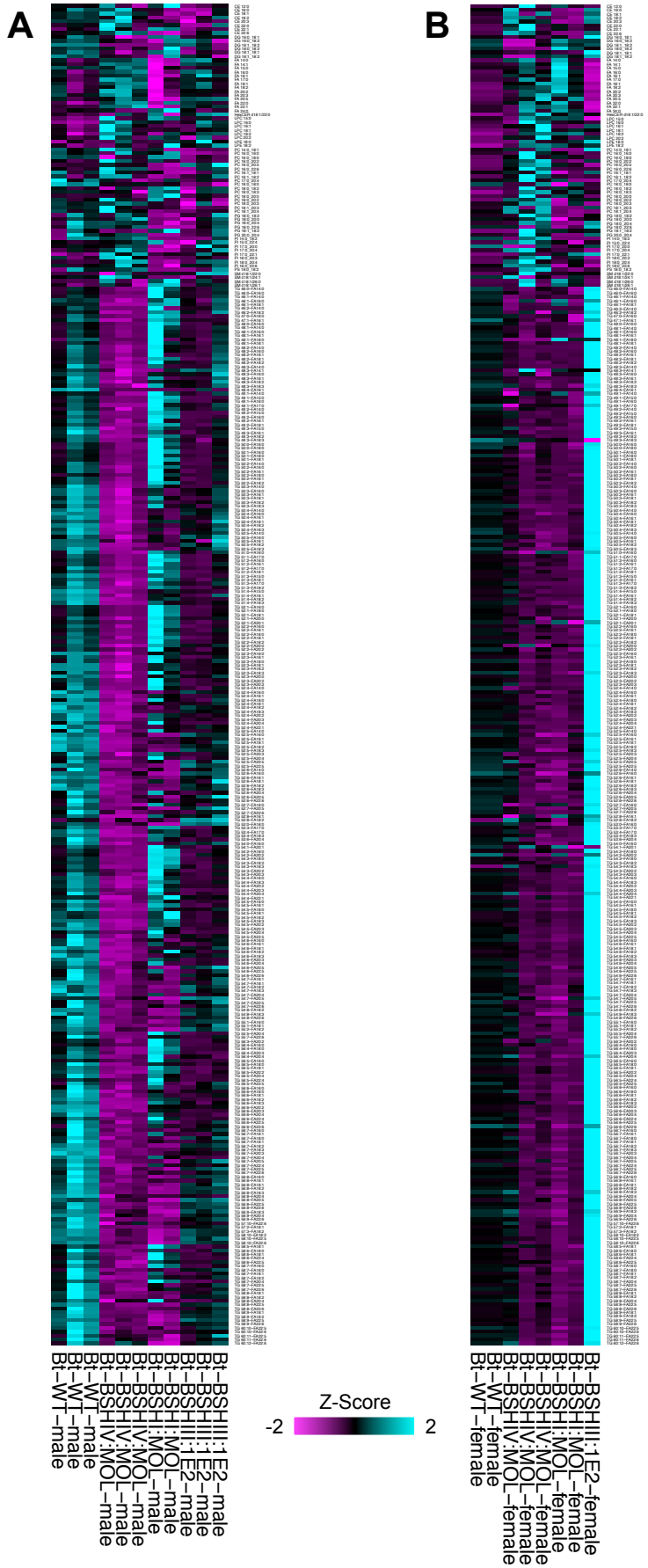
A
B
Bt−BSHIII:1E2−male
Bt−BSHIII:1E2−female
Bt−BSH:MOL−male
Bt−BSH:MOL−female
Bt−BSHIV:MOL−male
Bt−BSHIV:MOL−female
Bt−WT−male
Bt−WT−female
Z-Score
-2
2

888 **Supplementary Fig. 7. Sex differences in lipidomic response to *Turicibacter bsh* expression**
889 **in *B. thetaiotaomicron***. Similar to **Fig. 5b**, but animal lipidome analysis separated into **a**) males
890 and **b**) females. Note that lipid species presented were found to be significantly altered by
891 expression of at least one *bsh* in males and females combined (i.e. all lipid species shown across
892 the three analyses are the same). Each column represents one animal.
893

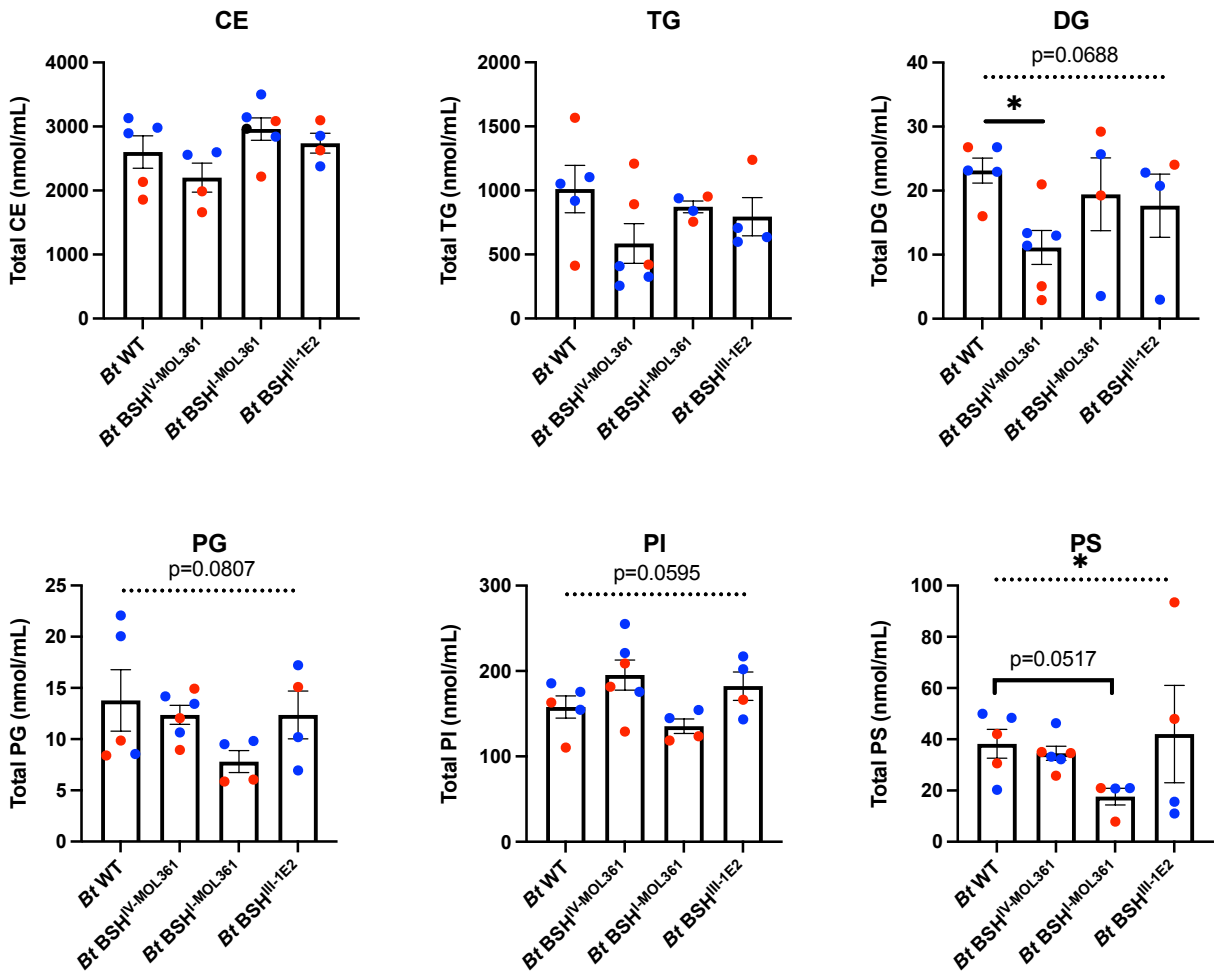

Supplementary Fig. 8. *Turicibacter bsh* expression by *B. thetaiotaomicron* is sufficient to drive broad scale changes in circulating host lipids in male and female mice. Related to **Fig. 6e-j**, circulating concentrations of specific lipid categories in mice colonized by *B. thetaiotaomicron* expressing the noted *Turicibacter bsh* homologs. Each point represents one animal, red points indicate female, blue represent male. n=4-5 per colonization, error bars represent mean +/- SEM. Statistical comparison done with Welch's ANOVA with Dunnet's multiple comparisons, dotted bar represents combined ANOVA statistic for each group versus the experimental mean, *p<0.05.